Evaluation of a computer model for biocide action against biofilms
by Sara Sherman Sanderson

A thesis submitted in partial fulfillment of the requirements for the degree of Master of Science in Chemical Engineering
Montana State University

Abstract:
The goal of this research was to evaluate a computer model for biocide action on biofilms in the context of biocide dosing and biofilm regrowth. The model incorporates bulk fluid and biofilm dynamics as well as reaction and diffusion of biocide and substrate. For evaluation, a series of annular reactor experiments was performed to obtain disinfection and regrowth parameters. The effect of applying monochloramine at various concentration and dose durations to Pseudomonas aeruginosa biofilms was determined.

Experiments demonstrated that disinfection and regrowth parameters varied as the dosing protocol changed. All experiments showed decreases in viable and total cell numbers. The higher dose (4 mg L-1) experiments showed approximately a 4 log reduction in viable cells soon after the dose was added. The lower dose (2 mg L-1) experiments showed less than 1 log reduction. For both protocols, the maximum total cell reductions, which came much later than the viable cell reductions, were near 1 log. All dosing protocols demonstrated a steady regrowth rate of viable cells at a rate slower than the maximum growth rate. The average regrowth rate was 0.103 ± 0.014 hr -1. The amount of effluent total chlorine appeared to depend on the amount of reactive biomass in the system. The 4 mg L-1 dose experiments showed a decrease in reactive biomass, while the 2 mg L-1 dose experiments showed an increase. Transport limitation of biocide was not a significant factor in these experiments. In double dose experiments, the effectiveness of the second dose was always less than the effectiveness of the first dose. The modeling results captured the overall trends seen in the experiments. There were many individual features, however, that the model could not adequately fit.

The experimental and modeling results indicate that more concentrated, shorter doses of monochloramine were more effective than the same amount of monochloramine delivered at lower concentrations over longer periods of time. When results from lower, longer dose experiments were fitted, the model parameters point toward a physiological response by the cells making them less susceptible to disinfection. The model and experiments both support timed dose strategies for efficient control.

EVALUATION OF A COMPUTER MODEL

FOR BIOCIDE ACTION AGAINST BIOFILMS

by

Sara Sherman Sanderson

A thesis submitted in partial fulfillment
of the requirements for the degree

of

Master of Science

in

Chemical Engineering

MONTANA STATE UNIVERSITY–BOZEMAN
Bozeman, Montana

April 1996

APPROVAL

of a thesis submitted by

Sara Sherman Sanderson

This thesis has been read by each member of the thesis committee and has been found to be satisfactory regarding content, English usage, format, citations, bibliographic style, and consistency, and is ready for submission to the College of Graduate Studies.

April 15, 1996
Date

Philip A. Stewart
Chairperson, Graduate Committee

Approved for the Major Department

April 16, 1996
Date

John T Sears
Head, Major Department

Approved for the College of Graduate Studies

4/21/96
Date

R K Brown
Graduate Dean

STATEMENT OF PERMISSION TO USE

In presenting this thesis in partial fulfillment of the requirements for a master's degree at Montana State University–Bozeman, I agree that the Library shall make it available to borrowers under rules of the Library.

If I have indicated my intention to copyright this thesis by including a copyright notice page, copying is allowable only for scholarly purposes, consistent with "fair use" as prescribed in the U. S. Copyright Law. Requests for permission for extended quotation from or reproduction of this thesis in whole or in parts may be granted only by the copyright holder.

Signature Sara Sherman Sanderson

Date April 15, 1996

ACKNOWLEDGMENTS

I would like to express gratitude to my research and academic advisor, Dr. Phil Stewart. He has provided exceptional guidance and insight for my graduate work. My committee members, Dr. John Sears and Dr. Martin Hamilton, also need acknowledging for their help and guidance.

The students and staff at the Center for Biofilm Engineering have made the last few years of my education very enjoyable. I would like to thank my friends there for some great times. A huge thank you goes to Dr. Ron Larsen and Mary Williams Huenergardt who made my first two summers in Montana absolutely wonderful. They are both extraordinary people and directly influenced my returning to the Center for graduate work.

I would like to thank my family for their continuous love, support, and encouragement. This goal could not have been accomplished without them.

A special thank you goes to my husband, Michael, for providing endless support and much love and happiness during these challenging years.

TABLE OF CONTENTS

TABLE OF CONTENTS—Continued

TABLE OF CONTENTS—Continued

LIST OF TABLES

LIST OF TABLES—Continued

LIST OF TABLES—Continued

LIST OF FIGURES

LIST OF FIGURES—Continued

ABSTRACT

The goal of this research was to evaluate a computer model for biocide action on biofilms in the context of biocide dosing and biofilm regrowth. The model incorporates bulk fluid and biofilm dynamics as well as reaction and diffusion of biocide and substrate. For evaluation, a series of annular reactor experiments was performed to obtain disinfection and regrowth parameters. The effect of applying monochloramine at various concentration and dose durations to *Pseudomonas aeruginosa* biofilms was determined.

Experiments demonstrated that disinfection and regrowth parameters varied as the dosing protocol changed. All experiments showed decreases in viable and total cell numbers. The higher dose (4 mg L^{-1}) experiments showed approximately a 4 log reduction in viable cells soon after the dose was added. The lower dose (2 mg L^{-1}) experiments showed less than 1 log reduction. For both protocols, the maximum total cell reductions, which came much later than the viable cell reductions, were near 1 log. All dosing protocols demonstrated a steady regrowth rate of viable cells at a rate slower than the maximum growth rate. The average regrowth rate was 0.103 ± 0.014 hr^{-1}. The amount of effluent total chlorine appeared to depend on the amount of reactive biomass in the system. The 4 mg L^{-1} dose experiments showed a decrease in reactive biomass, while the 2 mg L^{-1} dose experiments showed an increase. Transport limitation of biocide was not a significant factor in these experiments. In double dose experiments, the effectiveness of the second dose was always less than the effectiveness of the first dose. The modeling results captured the overall trends seen in the experiments. There were many individual features, however, that the model could not adequately fit.

The experimental and modeling results indicate that more concentrated, shorter doses of monochloramine were more effective than the same amount of monochloramine delivered at lower concentrations over longer periods of time. When results from lower, longer dose experiments were fitted, the model parameters point toward a physiological response by the cells making them less susceptible to disinfection. The model and experiments both support timed dose strategies for efficient control.

INTRODUCTION

A biofilm is composed of microbial cells and abiotic substances embedded in an extracellular polymeric substance matrix attached to a substratum (Characklis and Marshall, 1990). The abiotic particles may include silts, clays, precipitates, and corrosion products. A biofilm system would include the biofilm, the enveloping gas and/or liquid layers, and the substratum to which the biofilm is attached (Characklis and Marshall, 1990). The processes of microbial growth, death, diffusion, reaction, and detachment take place concurrently in the biofilm system.

Relevance of Biofilms

Biofilms can form on nearly any surface in contact with water. There are many positive uses of biofilms in the natural environment and engineered systems. Biofilms, for example, remove dissolved and particulate contaminants from natural streams and in wastewater treatment plants (Forster *et al.*, 1986; Ryhiner *et al.*, 1988; Characklis and Marshall, 1990). They are used to increase yield in metal and mineral extraction and improve productivity and stability of biotechnology processes (Norberg and Rydin, 1984; Geesey and Jang, 1989; Characklis and Marshall, 1990; Jang *et al.*, 1990). However, most attention focuses on the negative attributes of biofilm formation, particularly in industrial and medical systems.

Biofilms cause fouling of many industrial systems including heat exchangers and cooling water towers. The presence of biofilms in these systems results in energy losses and reduced performance (Suidan, 1986; Zelver, 1979; Characklis, 1981). They promote corrosion and biodeterioration of equipment and pipelines (Characklis and Marshall, 1990; Bremer and Geesey, 1991; Videla and Characklis, 1992; Geesey *et al.*, 1994; Lee *et al.*, 1994). Human lives are also impacted by biofilms in a more direct way. An example of this is found in the drinking water industry. Biofilms decrease water quality and contribute toward coliform outbreaks in drinking water distribution systems (van der Wende *et al.*, 1989; van der Wende and Characklis, 1990; Camper *et al.*, 1991; Camper, 1994). They also promote dental caries and periodontal disease by forming on teeth and gums (Costerton *et al.*, 1987). Biofilms cause recalcitrant infections associated with medical implants and catheters (Gristina *et al.*, 1985(a); Gristina *et al.*, 1985(b); Nickel *et al.*, 1985; Costerton *et al.*, 1987).

Mechanical cleaning and antimicrobial chemicals are generally used as the means of controlling biofilms in these systems. Mechanical cleaning techniques, however, are often difficult, impractical, and expensive. Antimicrobial chemicals such as biocides and antibiotics have therefore come to the forefront in control.

It is widely recognized that biofilms are more difficult to eradicate than their planktonic counterparts (Costerton et al., 1987; Nichols, 1989; Brown and Gilbert, 1993). The fundamental biological, physical, and chemical mechanisms underlying this increased resistance are not yet well understood. The challenge

is thus to elucidate these mechanisms so that biofilms can be effectively controlled. Engineering biofilm control through models by developing quantitative descriptions of the mechanisms is one way to meet the challenge.

Modeling allows for organization and integration of the complex biological, physical, and chemical processes occurring in biofilm systems. Figure 1, presented by Stewart *et al.* (1996), shows modeling being used to determine the effectiveness of alternative biocide dosing protocols. These model simulations demonstrate the idea that engineered dosing strategies can significantly increase the effectiveness of a biocide. Modeling allows for easy comparison of alternative strategies. Using engineering approaches to design biofilm control programs should lead to lower costs and less waste as optimum treatment protocols can be developed for various systems.

Research Goal and Objectives

The goal of the research presented in this thesis was to evaluate a computer model for biocide action on biofilms. The model was to be evaluated in the context of biocide dosing and biofilm regrowth. The objectives of this study were to:

1) Experimentally determine disinfection and regrowth parameters for biofilm treated with various biocide dose concentrations and dose durations.
2) Evaluate the capacity of a computer model to capture the qualitative and quantitative features of the experimental data.

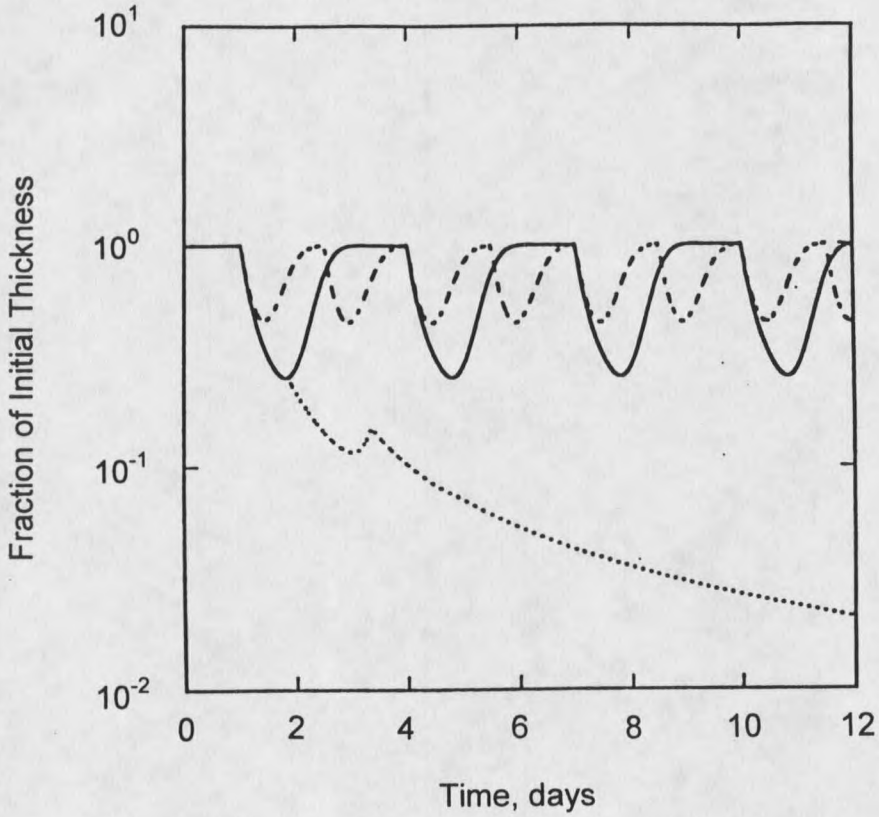

Figure 1. Alternative biocide dosing protocols. The normalized thickness, L_f/L_f°, is plotted for three alternative repeated treatments that begin at t = 1 day: 4 g m^{-3} for 1 hr repeated every 3 days (—); 2 g m^{-3} for 1 hr repeated every 1.5 days (---); 4 g m^{-3} at t = 1 day, followed by 0.5 g m^{-3} for 1 hr 0.8 days later, thereafter 0.5 g m^{-3} for 1 hr every 1.5 days (····).

LITERATURE REVIEW

Control of Biofilms with Antimicrobial Agents

Antimicrobial agents are a principal weapon used in the challenging task of biofilm control. Numerous oxidizing and nonoxidizing biocides are available for control purposes. Chlorine, an oxidizing biocide, has been used for decades and is still commonly used (Characklis and Marshall, 1990; Chen *et al.*, 1993; Griebe *et al.*, 1994). Chlorine is a popular biocide due to its availability and inexpensiveness (Chen *et al.*, 1993). However, chlorine's high reactivity and water's high chlorine demand limits the effectiveness of the biocide by deterring its actual penetration into the biofilm (LeChevallier *et al.*, 1988; van der Wende, 1991; de Beer *et al.*, 1994). There is also concern about chlorine's toxicity, possible reaction products, and promotion of chemical corrosion on various metals when using it for biofouling treatment. Alternative biocides are therefore receiving more attention.

Monochloramine is an alternative oxidizing biocide being used for control purposes. It is less reactive than free chlorine and thus thought to be able to better penetrate biofilms (LeChevallier *et al.*, 1988; Characklis and Marshall, 1990; Chen *et al.*, 1993). Griebe *et al.*, 1994 and Chen *et al.*, 1993 have shown that monochloramine was more effective than chlorine for inactivation of *Pseudomonas aeruginosa* biofilms. Monochloramine was the biocide chosen for

this project. It is prepared from chlorine and ammonia.

Mathematical Modeling

Mathematical modeling allows for integration and organization of the multiple simultaneous processes occurring when a biocide acts on a biofilm. It is a useful tool for testing hypotheses, interpreting data, and guiding experimental design.

The focus of this project is on a biofilm model incorporating disinfection with an antimicrobial agent. Validating such a model involves assessing the extent to which the model is well-founded and fulfills the purpose for which it was formulated (Hamilton, 1991). Model validation encompasses verification, sensitivity analysis, and evaluation (Hamilton, 1991). Evaluation, a comparison of the model's output to measurement of the real system, is what this project focuses on. There have been models developed for the investigation of planktonic disinfection and of biofilm growth and activity. Models that combine disinfection with biofilm processes are new and relatively untested.

Much of the past disinfection work focuses on using chlorine. There are models examining chlorine in drinking water systems (Al-Hoti *et al.*, 1990; Biswas *et al.*, 1993; Rossman *et al.*, 1994). The antimicrobial agent, ozone, which is beginning to be used more frequently, has been modeled for use in water treatment (Zhou *et al.*, 1994). There are also models looking at antibiotic penetration into biofilms (Nichols *et al.*, 1988; Nichols *et al.*, 1989). Most of the

disinfection models either fail to consider biofilms in their environments or incompletely consider the biofilm system, its processes and interactions.

Other models specifically address the processes and interactions occurring in a biofilm system. The models have developed over time from very simple models to more complex ones capturing the innate biofilm processes as knowledge and technology have progressed. The following processes, in various combinations, have all been the focus of models: growth, attachment, detachment, diffusion of substrate, diffusion of neutral and ionic species, reaction, adsorption, and transport in the bulk liquid (Rittman and McCarty, 1980; Gujer and Wanner, 1990; Skowland, 1990; Rittman and Manem, 1992; Flora *et al.*, 1993; Stewart, 1993; Flora *et al.*, 1995(a); Wanner and Reichert, 1996). The difficulty comes in coupling these processes for creating a model that can accurately predict behavior of biofilms in various environments. Efforts have been made in modeling a biofilm system to incorporate many of these processes. Various reactor systems, particularly those with activated carbon or other porous media, have been readily modeled (Chang and Rittman, 1987; Skowland and Kirmse, 1989; Coelhoso *et al.*, 1992; Jones *et al.*, 1993; Flora *et al.*, 1995(b); Wanner et al., 1995).

Disinfection models do not necessarily include biofilms, while biofilm models do not readily allow for disinfection processes. For biofilm control, a model of systems of varying environments and geometries that can incorporate the fundamental processes along with the addition of an antimicrobial agent is

desired. There has been some work done recently by Stewart *et al.* (1996) and Stewart (1994) using biocides and antibiotics in a model of biofilm accumulation. This model does allow for antimicrobial action against biofilms. The model evaluated in this project also allows for antimicrobial action on biofilms to be examined. The mathematical model evaluated was implemented using AQUASIM.

AQUASIM was developed at the Swiss Federal Institute for Environmental Science and Technology (Reichert,1994(b)). It is a simulation and data analysis program designed for modeling aquatic systems. The user can compose the spatial configurations of an aquatic system out of different compartments, which are connected by links. There is flexibility in specifying the transformation processes. AQUASIM allows the user to not only perform simulations, but also sensitivity analyses, parameter estimations, and uncertainty estimations. The biofilm accumulation model described by Stewart *et al.*, 1996 can perform corresponding simulations using a different interface. AQUASIM can couple the processes from the disinfection and biofilm models into a single, user-friendly program. Using this program, a simulation of antimicrobial action on biofilms in varying environments can easily be performed.

THEORY

Mathematical Model

A phenomenological model of biofilm dynamics was implemented using AQUASIM. The program has the capacity needed to model disinfection of a biofilm with an antimicrobial agent. There is a biofilm reactor compartment in the program. This compartment represents a well mixed reactor with biofilm growing on the walls (Reichert, 1994(a)). For describing processes, this compartment can be divided into two zones, a bulk liquid zone and a biofilm zone. The bulk liquid zone simulates a well-mixed, constant volume, continuous flow reactor. For the biofilm zone, the model averages the biofilm structure and properties over planes parallel to the substratum resulting in a uniformly thick planar biofilm changing only in the direction perpendicular to the substratum. The two zones are separated by a boundary layer, which manifests itself by a diffusive mass transfer resistance (Reichert, 1994(b)). A one-dimensional mathematical model is used to describe the biofilm reactor compartment. The population dynamics and concentration gradients of dissolved substances within the biofilm are calculated according to equations proposed by Gujer and Wanner (1990) (Reichert, 1994(a)). Bulk flow in and out of the reactor, growth of the biofilm, cell detachment, diffusion of dissolved solutes into the biofilm, production and consumption of dissolved solutes, and disinfection are all accounted for.

Differential material balances with terms for these processes are found in the 1-D mathematical model. The balances on the zones within the biofilm reactor compartment will be separately elaborated on in the following sections.

Biofilm Zone

A single species biofilm is considered for this project. However, a multispecies model is needed since there are two cell states, live and dead. A volume fraction is used to describe the concentration of cells in the biofilm. This fraction of all cells, live and dead, stays constant thus resulting in the balance

$$x_T = x_A + x_I \tag{1}$$

Intrinsic cell density, ρ_x, is used for conversion from volume fraction to mass units. Processes affecting living cells in the biofilm include: growth, advection, and disinfection. Initially the biofilm is only composed of live cells. The balance on live cells is

$$\frac{\partial x_A}{\partial t} = \frac{\mu_{MAX}\, S}{K_s + S}\, x_A - \frac{\partial}{\partial z}(v\, x_A) - k_{dis}\, B\, x_A \tag{2}$$

with initial conditions

$$x_A = x_T \quad at\ t = 0 \quad for\ 0 \le z \le L_f^{\circ} \tag{3}$$

The terms in equation (2) from left to right represent accumulation, growth, advection, and disinfection. Monod kinetics describe microbial growth. Cells displace their neighbors as they grow thus creating cell volume.

Cells at the same point in the biofilm move with the same velocity whether they are live or dead. The advective velocity is

$$\frac{\partial v}{\partial z} = \frac{\mu_{MAX}\, S}{K_s + S}\,\frac{x_A}{x_T} \qquad (4)$$

with boundary condition

$$v = 0 \quad at\ z = 0 \quad for\ t > 0 \qquad (5)$$

The thickness of the biofilm changes by growth and detachment of cells

$$\frac{dL_f}{dt} = v|_{z=L_f} - k_d\, L_f^2 \qquad (6)$$

with initial condition

$$L_f = L_f^{\circ} \quad at\ t = 0 \qquad (7)$$

A steady state biofilm, in which growth and detachment are equal, is attained before biocide dosing occurs.

A reaction-diffusion equation is used to describe the concentration of the

growth limiting substrate

$$\frac{\partial S}{\partial t} = D_s \tau \frac{\partial^2 S}{\partial z^2} - \frac{\mu_{MAX}}{Y_{xs}} \frac{S}{K_s + S} x_A \rho_x \qquad (8)$$

with initial condition

$$S = S^i \quad at\ t = 0\ for\ 0 \le z \le L_f^\circ \qquad (9)$$

Only live cells in the biofilm consume substrate. Molecular diffusion is the transport mechanism for dissolved species in biofilm. The parameter, τ, allows for reduction in the effective diffusion coefficient inside the biofilm.

Boundary conditions include a matching flux condition at the biofilm-bulk fluid interface

$$\tau \frac{\partial S}{\partial z}\Big|_{z=L_f} = \frac{S^* - S|_{z=L_f}}{L_L} \quad for\ t \ge 0 \qquad (10)$$

and a no-flux condition at the substratum

$$\frac{\partial S}{\partial z}\Big|_{z=0} = 0 \quad for\ t \ge 0 \qquad (11)$$

The biocide reacts with the biofilm and is subject to a reaction-diffusion interaction. The balance on biocide is

$$\frac{\partial B}{\partial t} = D_b \tau \frac{\partial^2 B}{\partial z^2} - k_{rxn} B N \quad (12)$$

The biocide reacts equally with live and dead cells. The initial and boundary conditions are

$$B = 0 \quad at\ t = 0\ for\ 0 \le z \le L_f^\circ \quad (13)$$

$$B = B^* \quad at\ z = L_f\ for\ t > 0 \quad (14)$$

$$\frac{\partial B}{\partial z} = 0 \quad at\ z = 0\ for\ t > 0 \quad (15)$$

Neutralizer in the biofilm consumes biocide. The balance on neutralizer in the biofilm is

$$\frac{\partial N}{\partial t} = 0.0417 \frac{\mu_{MAX} S}{K_s + S} X_A - \frac{k_{rxn} B N}{Y_{bn}} \quad (16)$$

with initial condition

$$N = N^\circ \quad at \quad t = 0 \quad for \quad 0 \le z \le L_f^\circ \quad (17)$$

Bulk Fluid Zone

The balances for the bulk fluid zone consider the influent and effluent flows from the reactor, the bulk phase reactions, and net reaction from the biofilm.

The balance on live cells is

$$\frac{dX_A^*}{dt} = \frac{\mu_{MAX}\, S^*}{K_s + S^*} X_A^* - k_{dis}\, B^*\, X_A^* + k_d\, x_A|_{z=L_f}\, \rho_x\, L_f^2\, \frac{A}{V} - \frac{Q}{V} X_A^* \qquad (18)$$

A similar balance is derived for dead cells, except there is no growth

$$\frac{dX_I^*}{dt} = k_{dis}\, B^*\, X_A^* + k_d\, x_I|_{z=L_f}\, \rho_x\, L_f^2\, \frac{A}{V} - \frac{Q}{V} X_I^* \qquad (19)$$

where there are initially no cells in the reactor

$$X_A^* = X_I^* = 0 \quad at\ t = 0 \qquad (20)$$

The influent continually adds substrate to the system, which is consumed in the bulk fluid and the biofilm. The balance on substrate is

$$\frac{dS^*}{dt} = \frac{Q}{V}(S^i - S^*) - \frac{\mu_{MAX}\, S^*}{K_s + S^*} X_A^* - D_s\, \tau\, \frac{dS}{dz}|_{z=L_f}\, \frac{A}{V} \qquad (21)$$

with initial condition

$$S^* = S^i \quad at\ t = 0 \qquad (22)$$

The biocide is added by a step procedure. The resulting balance in the bulk fluid is

$$\frac{dB^*}{dt} = \frac{Q}{V}(B^i - B^*) - D_b \tau \left.\frac{dB}{dz}\right|_{z=L_f} \frac{A}{V} \quad \textbf{(23)}$$

with a step dose condition of

$$B^i(t) = 0 \quad t < t_1 \quad \textbf{(24)}$$

$$B^i(t) = B^i \quad t_1 \le t \le t_2 \quad \textbf{(25)}$$

$$B^i(t) = 0 \quad t > t_2 \quad \textbf{(26)}$$

with

$$B^* = 0 \quad at\ t = 0 \quad \textbf{(27)}$$

METHODS

Microbial Species

Pseudomonas aeruginosa ERC 1 was used in pure culture in the work. *P. aeruginosa* is a facultative aerobic chemoorganotroph capable of denitrification (Krieg and Holt, 1984; Brock and Madigan, 1991). It is a Gram-negative rod approximately 0.5 to 0.7 μm by 1.5 to 3.0 μm. Motility is attained through polar monotrichous flagellation. It can grow in temperatures from 4°C to 43°C with the optimum temperature being 37°C. The optimal pH is 6.8.

P. aeruginosa is found in natural aquatic environments. It is known to readily form biofilms (Bakke *et al.*, 1984). There have been extensive studies performed on both the planktonic and biofilm cells (Trulear, 1983; Bakke *et al.*, 1984). Growth kinetics and stoichiometric coefficients have been previously determined (Robinson *et al.*, 1984; Bakke *et al.*, 1984).

Nutrient Medium and Phosphate Buffer

The *P. aeruginosa* were grown on a minimal salts medium with glucose as the sole carbon source. The nutrient medium, excluding the glucose, and the phosphate buffer solutions were prepared in 11 L Nalgene containers. These containers were autoclaved at 121°C for 6 hrs. A concentrated glucose solution was added by injection through a septum. During injection, the glucose solution

was filter-sterilized through a 0.2 μm filter (Disposable Sterile Syringe Filter, Corning Glassworks, Product No. 21052-25). The constituents of the nutrient medium and phosphate solution are listed in Table 1. The nutrient medium is modified from Brent Peyton's (1992) medium formula in that it does not contain added calcium. This was done to prevent calcium precipitation.

Table 1. Influent nutrient medium and phosphate buffer solution formulas.

Nutrient Medium:	
Substance:	Concentration: (g m^{-3})
Glucose	20.0
$MgSO_4 \cdot 7H_2O$	2.0
KNO_3	20.0
$(NH_4)_6Mo_7O_{24} \cdot 4H_2$	0.0014
$ZnSO_4 \cdot 7H_2O$	0.142
$MnSO_4 \cdot H_2O$	0.0114
$CuSO_4 \cdot 5H_2O$	0.0028
$Na_2B_4O_7 \cdot 10H_2O$	0.0014
$FeSO_4 \cdot 7H_2O$	0.159
$(HOCOCH_2)_3N$	0.200
$Co(NO_3)_2 \cdot H_2O$	0.0023
Phosphate Buffer:	
Substance:	Concentration: (g m^{-3})
Na_2HPO_4	95.5
KH_2PO_4	102.0

Monochloramine Stock Solution

A monochloramine stock solution was prepared for each experiment. A pH 8.9 solution was initially prepared by adding 0.5 g K_2HPO_4 to 1 L of double distilled water. This solution was autoclaved for 30 min at 121°C and then cooled. 0.22 g of NH_4Cl was dissolved in 200 mL of the pH 8.9 solution using a stir bar. 2 mL of Clorox® regular bleach was then slowly added to this solution and mixed for 5 min. This stock solution was stored at 4°C for 1 hr to complete the reaction. Double distilled water was used to dilute the stock to the required concentration.

Annular Reactor System

The annular reactor (RotoTorque) is an important tool for biofilm research. The annular reactor is a continuous flow stirred tank reactor (CFSTR) (Figure 2). It consists of two polycarbonate cylinders, an outer stationary cylinder and a co-axial rotating inner cylinder. Four vertical draft tubes are found in the inner cylinder. They are angled so that rotation of the cylinder drives fluid through the tubes and provides vertical mixing. The reactor can thus be considered well mixed (Trulear, 1983). There should be no concentration differences existing in the bulk fluid. Rotation of this inner drum also imposes a shear stress on the outer cylinder wall. This shear stress should be uniform since the space

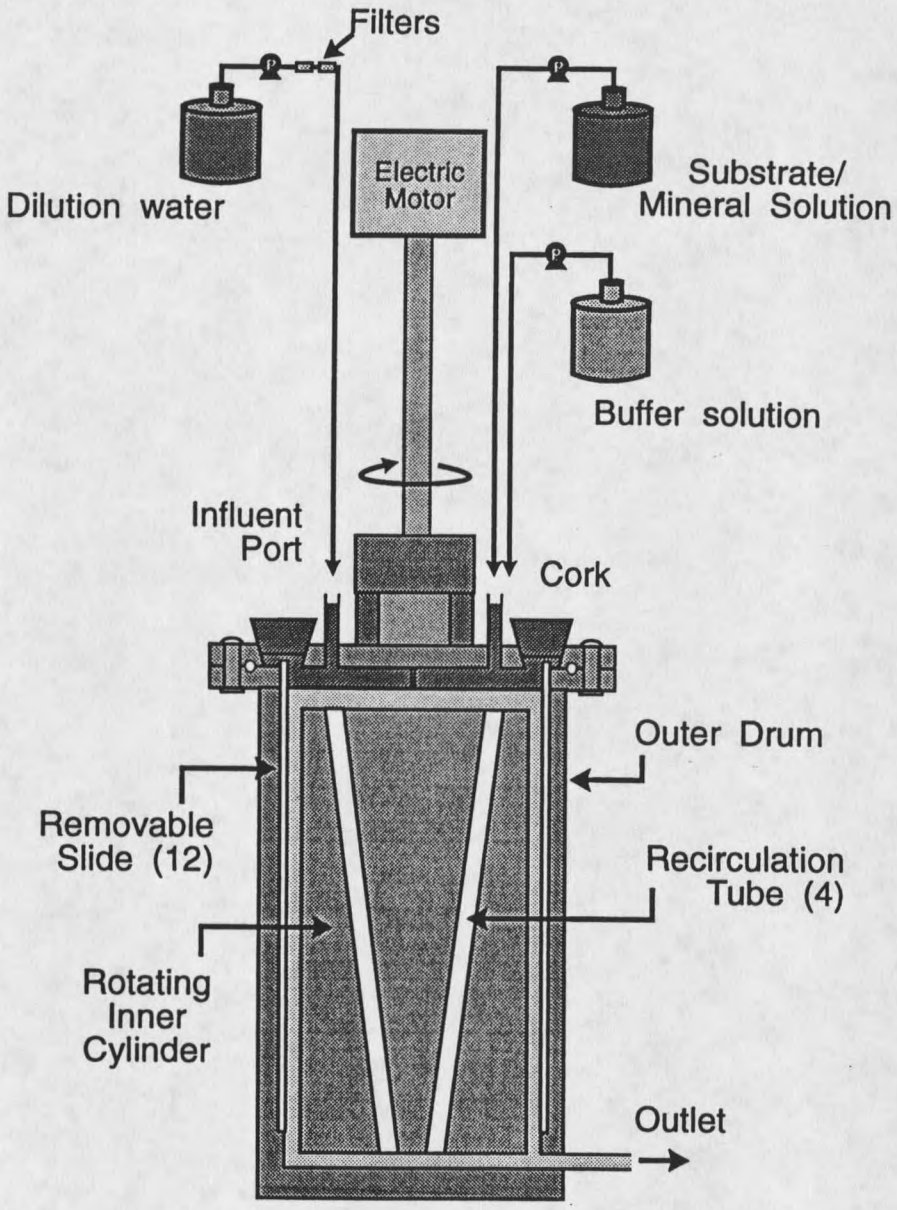

Figure 2. Schematic of annular reactor system.

between the cylinders is constant (Drury, 1992).

The inside wall of the outer cylinder had a biofilm growth area of 7.81×10^{-2} m^2. There were twelve vertical grooves cut into this wall. Stainless steel removable slides were placed into these slots. The slides each had an area of approximately 3.74×10^{-2} m^2. They allowed for direct sampling of biofilm while keeping the system on line. The slides were removed through rubber-stoppered holes on the top of the reactor. The biofilm growth on these slides was assumed to be relatively uniform due to the ideal mixing and constant shear stress. Large amounts of biomass were able to be produced at relatively low volumetric flow rates with minimum growth of suspended organisms. A detailed description of the annular reactor is given in Appendix A.

Start-up, Operation, and Sampling Methods

The annular reactor system is cleaned by scrubbing the reactor and slides with hot water and "Micro" lab soap. The reactor is assembled with the slides in the grooves, all influent and effluent tubing (Masterflex 6411 -15, -16; 6485-16; 96400 -15, -25) attached, and all flow meters and dilution water filters in line. The open tubing ends were covered with aluminum foil. The reactor was autoclaved for 0.5 hr at 121°C and cooled. After cooling, the glucose substrate, phosphate buffer, and dilution water sources were attached through sterile connectors. Dilution water was filter sterilized by passing it through two Gelman capsule filters (0.2 μm, Product No. 12112) in series. Three peristaltic pumps

(Masterflex 7553-30, Cole-Parmer Instrument Company) with pumpheads (Masterflex 7014, 7016) were used to fill the reactor in a 1:1:10 mixture of the three solutions.

After filling the reactor, the flow was halted and rotation of the inner cylinder initiated at a speed of 150 rpms. 10 mL of frozen stock culture (10^8 cells mL^{-1}) of *P. aeruginosa* was allowed to thaw from -60°C to room temperature. Inoculation of the reactor with the bacteria occurred by pouring the stock through a rubber-stoppered hole in the top of the reactor. The bacteria were then grown in batch for 24 hrs. After this incubation period, the influent flows were restarted. The cumulative flow rate for the reactor was set at 19.2×10^{-4} m^3 hr^{-1} (32 mL min^{-1}) with a hydraulic residence time of 0.34 hr. The individual flows are as follows: glucose substrate, 6×10^{-5} m^3 hr^{-1} (1 mL min^{-1}); phosphate buffer, 6×10^{-5} m^3 hr^{-1} (1 mL min^{-1}); dilution water, 1.8×10^{-3} m^3 hr^{-1} (30 mL min^{-1}). The reactor system was run at room temperature.

Biofilm covered slides were removed through the rubber-stopped ports on the top of the reactor. Aseptic sampling was performed by disinfecting the stoppers and surroundings with a 200 mg L^{-1} chlorine solution and creating an upward draft with a nearby bunsen burner. The rubber stopper was removed after this treatment and the slide removed with sterile needle-nose pliers. The port was sealed with the stopper after quickly flaming the stopper end. The biofilm was scraped into 100 mL of the phosphate buffer which also contained 0.1 percent sodium thiosulfate. The sodium thiosulfate was added to neutralize the chlorine

to prevent further reaction with the biofilm. The solution was then homogenized for 2 min on full power using a tissumizer (Tekmar Co., Typ. T25 S1; TR-10 Power Control). A serial dilution was performed on the bacterial solution.

Effluent from the reactor needed to be sampled for number of viable bacteria, contamination, and chlorine present. Effluent samples were easily obtained through a three-way stopcock that had been placed in the effluent tubing. The stopcock was turned to divert flow to sampling receptacles when desired.

Monochloramine Addition

Monochloramine was added at specified dose concentrations and durations depending upon the experiment. It was added by a step procedure after seven days growth of the biofilm. A step addition maintained the concentration of biocide entering the reactor at the initial concentration over the entire dose duration. The monochloramine was prepared as previously described. It was diluted to the necessary concentration for maintaining the desired dose over the specified time period at the certain flow rate. The solution was placed in a beaker and capped by a rubber stopper with tubing through it. The monochloramine tube was plumbed, through a sterile connector, to the same flow line through which the phosphate buffer was added to the reactor. The buffer flow was clamped and the biocide flow opened at a desired time. The pump or tubing did not have to be readjusted by using this procedure. The flow of biocide was timed and clamped off and the buffer reintroduced to the system

after the specified dose duration.

Analytical Methods

Viable Cells

The number of viable cells in the biofilm was determined by serial dilution and plating of the homogenized cell suspension described in the sampling method. The phosphate buffer solution described in Table 1 was used for dilution. The dilutions were plated on Difcobacto R2A™ agar in triplicate using the drop plate method. The drop plate method is a procedure in which 10 μl drops of a particular dilution are dropped onto a plate. The resulting number of colonies per drop are converted to obtain counts in cfu mL^{-1}. Plates were incubated at 35°C for 24 hrs.

Total Cells

For determining total cells in the biofilm, certain dilutions (depending on the experiment performed) of cell suspensions were saved and 0.03 percent formalin added to the sample for preserving cells. A black nucleopore polycarbonate membrane (pore size 0.2 μm and 25 mm in diameter, Poretics Corporation, Cat. No. 11021) was then placed on cell free glass Millipore filter apparatus and rinsed with cell free water. 1 mL of the fixed cell suspension was slowly placed on this filter. 0.1 mL of 0.02 percent acridine orange was added and allowed to stain for 10 min. The solution was removed by applying a

vacuum and rinsed with approximately 1 mL of water. A drop of oil (R. P. Cargille Laboratories, Inc., non-drying immersion oil type FF) was placed on a microscope slide. The filter was gently put on top of this drop. Another drop of oil was put on top of the filter and covered with a glass cover slip. The slide was then examined under ultraviolet illumination on the Olympus BH2 epifluorescence microscope. The total number of bacteria in a field on the filter were counted using the field defined by the microscope eye-piece grid. 10 or more grid fields were observed each time for a total of 400 or more cells counted.

Viable Cell and Contamination Check of Reactor Effluent

Approximately 10 mL of reactor effluent was collected and homogenized for 1 min using the tissumizer. A serial dilution in phosphate buffer was performed. Various dilutions were then plated using the drop plate method on Difcobacto R2A™ agar. The plates were incubated at 35°C for 24 hr. The number of suspended organisms was determined. Plates were examined for evidence of contamination.

Chlorine Analysis

5 mL of reactor effluent were collected for chlorine analysis. N,N-diethyl-p-phenylenediamine (DPD) Total Chlorine Reagent Powder (HACH Co., Permachem™ Reagents) was added to the effluent sample. The powder was dissolved by shaking and allowed to react for 0.5 min before testing. A

spectrophotometer (Spectronic 601 Spectrophotometer, Milton Roy) was used for evaluation of the amount of chlorine present in the sample. To do this, the spectrophotometer was first calibrated for chlorine measurement (Clesceri et al., 1989). The spectrophotometer was used to read the absorbance at 515 nm. The concentration of chlorine in the sample was then calculated by multiplying it by a previously determined constant.

Interpretation of Experimental Data using AQUASIM

The biofilm disinfection and regrowth data was imported into AQUASIM for interpretation. This data was imported through the use of real list variables. These data pairs were basically used as target quantities for estimation of parameters. For fitting the model to experimental results, certain parameters were adjusted. The parameters were constant variables and could be estimated by the program with the help of the measured data or could be manually adjusted. The parameter estimation component of the model used the weighted least squares estimation method. This method determines parameter values by minimizing the function χ^2 according to the following equation

$$\chi^2(\boldsymbol{p}) = \sum_{i=1}^{n} \left(\frac{\boldsymbol{f}_{meas,i} - \boldsymbol{f}(\boldsymbol{p})}{\sigma_{meas,i}} \right)^2 \qquad \textbf{(28)}$$

The parameters adjusted in this project were the reaction coefficient, k_{rxn}, the disinfection coefficient, k_{dis}, and the yield coefficient of neutralizer, Y_{bn},

respectively.

These parameters were all found in the dynamic processes added to the program. The dynamic processes represent the interactions within the system important on a time scale. They allow for transformation of substances in fixed stoichiometric ratios. The dynamic processes have a process rate and stoichiometric coefficients that give a factor by which the process rate is multiplied to give rate of change of the substance (Reichert, 1994(b)). During the simulation, the dynamic processes only affected the variables. These variables, in turn, were used in the previously described balances for the biofilm reactor compartment. The process rates were set up in the model as growth, disinfection, and consumption. The growth process rate was

$$r_{growth} = \frac{\mu_{MAX}\, S}{K_s + S}\, x_A \qquad \textbf{(29)}$$

The stoichiometric coefficients for the growth rate process were 1 and 0.0417 for the live cell volume fraction and neutralizer, respectively. The process rate for disinfection was

$$r_{dis} = k_{dis}\, B\, x_A \qquad \textbf{(30)}$$

The stoichiometric coefficients were -1 and 1 for the live and dead cell volume fractions. Consumption had the following process rate in the model

$$r_{rxn} = k_{rxn} B N \quad (31)$$

The stoichiometric coefficients for this rate were -1 for biocide concentration and $-1/Y_{bn}$ for neutralizer concentration. Manipulation of k_{rxn}, k_{dis}, and Y_{bn} within this framework allows for more accurate fits when using the model. The values for all the parameters used in AQUASIM and their sources can be found in Table 8 in the results chapter.

EXPERIMENTAL DESIGN

The work in this research project can be divided into two areas: annular reactor experimental studies and mathematical model studies. The annular reactor studies consisted of core experiments and double dose experiments. The core experiments were completed first in the project. The results from this work were used in the simulations. The double dose experiments were then performed. In the annular reactor studies, viable and total cell counts and effluent total chlorine were measured. The reaction and transport of the monochloramine was analyzed. Similar analyses were done with the model simulations.

Annular Reactor Experimental Studies

A series of core annular reactor experiments with varied concentration and dose durations were performed. The range of doses was chosen to effect a wide range in degrees of disinfection. A control experiment, in which phosphate buffer was added instead of monochloramine, was included in the core experiments. The following table gives the core experiments along with the concentration and duration of the dose used for that experiment.

Table 2. Core experiments.

Experiment #	Dose Concentration, mg L^{-1}	Dose Duration, hr
3	4	2
4	4	2
6	0	2
10	2	4
12	2	8
14	4	4

After obtaining results from these core experiments, double dose experiments using combinations of the dosing protocols from the core experiments were performed. The differences in the double dose experiments were in the time between doses and in the concentration of the first dose. Table 3 gives an overview of these experiments.

Table 3. Double dose experiments.

Exp. #	1^{st} Dose		2^{nd} Dose		Time Between Doses, hr
	Conc., mg L^{-1}	Dur., hr	Conc., mg L^{-1}	Dur., hr	
17	4	2	4	2	40
18	2	4	4	2	0
19	4	2	4	2	60

The first double dose experiment, experiment #17, was performed with the intent of evaluating the difference between an *a priori* model prediction and the actual experiment. The last two double dose experiments were performed to

further investigate interesting trends seen in the core experiments. Experiments not listed were aborted for various reasons. Experiments #1, #2, #5, and #15 were ended due to mechanical difficulties such as leaks, loose slides in the reactor, pumping problems, or tubing problems. Experiments #7, #8, #9, and #11 were aborted due to contaminated systems. Experiments #13 and #16 were aborted due to an incorrect amount of chlorine being added to the system.

The viable cell counts for each experiment were obtained in colony forming units (cfu) per slide. This was converted to cfu per m^2 and put on a log scale for analysis. Total cells were similarly counted in cells per slide and converted to cells per m^2. They were put on the same log scale as the viable cell counts.

The effluent total chlorine measured was converted from the spectrophotometer absorbance reading to mg L^{-1} by using a previously determined constant. Since monochloramine was the only chlorine in the system and there is no strong oxidant, the effluent total chlorine concentration represents the concentration of monochloramine in the system.

The overall reaction rate of the monochloramine with the biofilm was examined using the following equation

$$V \frac{dB^*}{dt} = Q\,(B^i - B^*) - r_B \qquad \textbf{(32)}$$

The effluent total chlorine data was used for this analysis. The change in bulk monochloramine concentration with time was found at each data point. This change was calculated by averaging the change from the preceding points to the

desired point and from the desired point to the following point. The changes at the maximum and end points were determined by using only the concentration change with time from the preceding point to the maximum or end point. Calculations were not performed for the initial data points. The reaction rates were obtained using equation (32) after these calculations.

The transport limitation of the monochloramine in the biofilm was looked at by calculating an observable modulus according to the following equation (Bailey and Ollis, 1977)

$$\Phi = \frac{R_{OBS}\, L_f^2}{B^*\, D_B} \qquad \textbf{(33)}$$

where

$$R_{OBS} = \frac{r_B}{A\, L_f} \qquad \textbf{(34)}$$

The observable modulus was calculated at three points during the biocide dose corresponding to a one quarter, one half, and three quarters of the duration.

Mathematical Model Studies

The experimental results obtained for the core experiments were imported into AQUASIM. Within the model, the parameters k_{rxn}, k_{dis}, and Y_{bn} were adjusted using the parameter estimation component of the program until a reasonable fit

was obtained. Manual rounding of the parameters was done. Each experiment was examined individually. After the model was integrated for the core experiments, a prediction was made for a double dose experiment, experiment #17, using the parameters extracted from experiments #3 and #4. This experiment was then performed and a comparison of the experimental results to those predicted by the model was done. The monochloramine gradients in the biofilm could also be simulated to visualize extent of transport limitation inside the biofilm.

STATISTICAL METHODS

Each experiment was analyzed individually. Cell counts were transformed to the log scale before doing statistical calculations. Total chlorine concentrations were not transformed. The mean of replicate observations and the standard error of the mean (SEM) were calculated. The SEM measures the reliability of the observed mean as an estimate of the true mean (Miller *et al.*, 1990).

For each experiment, the mean and associated SEM were calculated for both the viable and total cell data. The mean and SEM for the effluent total chlorine were only calculated for experiments #18 and #19, the only experiments in which duplicate chlorine samples were taken.

Let Var_i denote the sample variance of N_i replicate $\log_{10}$ counts at the i^{th} of I time points in an experiment. Let VAR denote the mean of Var_1, ..., Var_I and let $SD = VAR^{0.5}$. The SD measures the variability among replicate counts on the log scale. The SEM for the mean of $\log_{10}$ counts at the i^{th} time point is then

$$SEM_i = \frac{SD}{\sqrt{N_i}}, \quad i = 1, \ldots, I \qquad \textbf{(35)}$$

The SEM values were used to construct error bars for means when the data were plotted. Note that the error bars around the means are quite narrow. All of the time effects summarized below are statistically significant. A tabulation of the means and associated SEMs are located in Appendix B.

RESULTS

The results of the annular reactor and mathematical model studies will be presented in this section. The raw data for this work is located in Appendix B through Appendix D.

Annular Reactor Studies

In all, 19 experiments were performed in the annular reactor studies. Nine of these were fully completed without experiment-ending complications. Viable and total cells, and effluent total chlorine were monitored for all experiments. The reaction rate of the monochloramine and extent of its transport limitation within the biofilm were determined.

Viable and Total Cells

The changes in viable and total cell numbers with time demonstrate the effect of the monochloramine on the *P. aeruginosa* biofilms. Figures 3 and 4 show the results from experiments #3 and #4. The same dosing conditions were used for these experiments to demonstrate the reproducibility of the annular reactor experiments. Good reproducibility was attained for these experiments. These figures both show an initial sharp 4 to 5 log decrease in viable cell numbers within the first 4 hrs after monochloramine was added. A log reduction is defined as the reduction of an initial density N_o (count m^{-2}) to N_1 (count m^{-2}) with the log

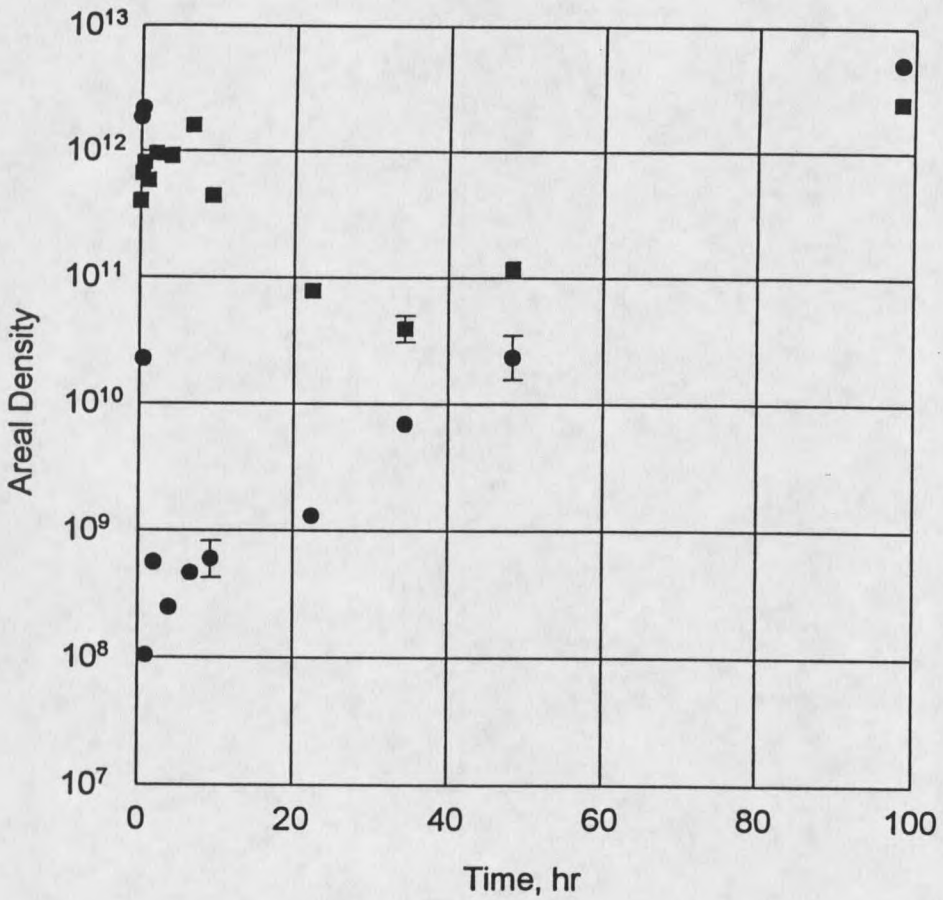

Figure 3. Experiment #3: 7-day old *Pseudomonas aeruginosa* biofilm treated with 4 mg L^{-1} monochloramine for 2 hr. Viable cell, cfu m^{-2}, (●) and total cell, cells m^{-2}, (■) areal densities vs. time. Error bars are shown on three points to indicate the statistical reliability of the plotted means. The first error bar on a viable cell point represents the SEM for 3 dilutions. The second error bar on a viable cell point represents the SEM for 2 dilutions. The total cell error bar represents the SEM for 10 fields counted.

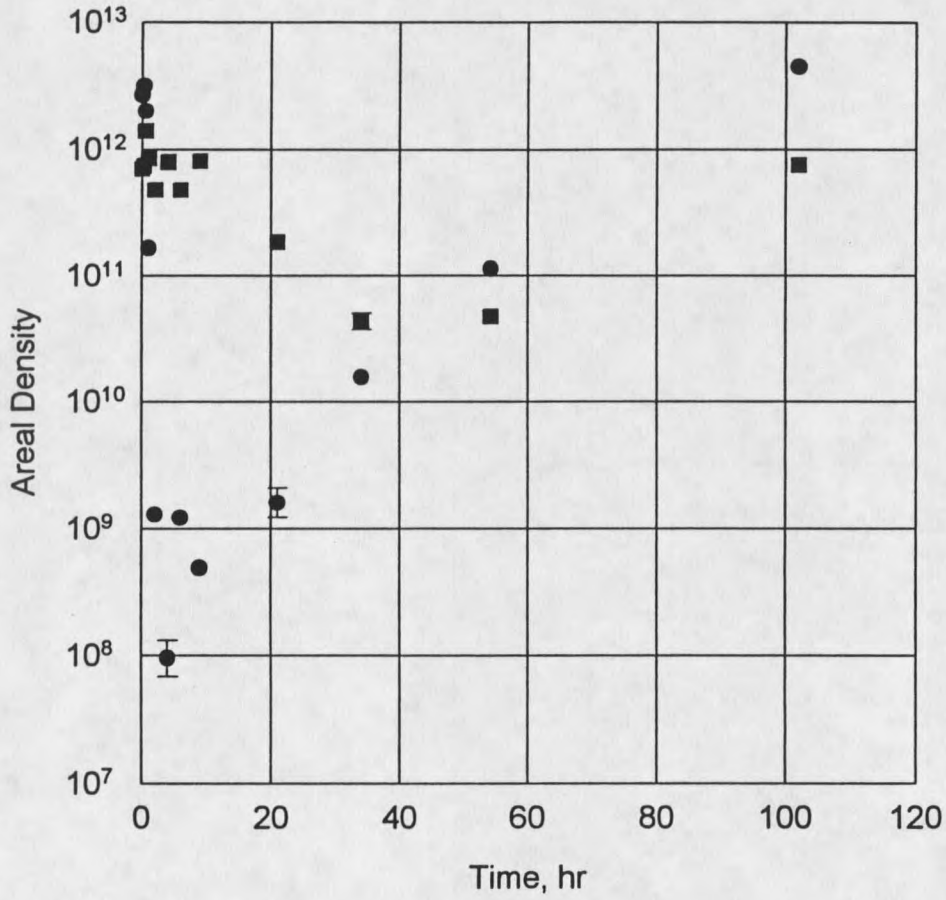

Figure 4. Experiment #4: 7-day old *Pseudomonas aeruginosa* biofilm treated with 4 mg L^{-1} monochloramine for 2 hr. Viable cell, cfu m^{-2}, (●) and total cell, cells m^{-2}, (■) areal densities vs. time. Error bars are shown on three points to indicate the statistical reliability of the plotted means. The first error bar on a viable cell point represents the SEM for 2 dilutions. The second error bar on a viable cell point represents the SEM for 3 dilutions. The total cell error bar represents the SEM for 10 fields counted.

reduction calculated as $-\log(N_1/N_o)$. Table 4 presents the maximum reductions in viable and total cells and the times that these minimum values were seen for all the completed experiments.

Table 4. Maximum reduction in biofilm total and viable cell numbers (log scale).

Experiment #	Maximum Log Reduction		Time After Dose of Minimum Values, hr	
	Total Cells, cells m^{-2}	Viable Cells, cfu m^{-2}	Total Cells, cells m^{-2}	Viable Cells, cfu m^{-2}
3	1.61	4.33	34.3	1.0
4	1.51	4.52	34.0	4.0
6	0.44	0.62	6.33	6.33
10	0.26	0.45	4.0	2.0
12	0.85	0.90	6.0	12.2
14	0.87	5.28	10.3	22.0
17 - 1st Dose	0.61	3.16	39.5	15.0
17 - 2nd Dose	0.76	1.65	63.5	12.0
18 - 1st Dose	0.18	0.78	3.75	3.75
18 - 2nd Dose	0.65	1.93	20.0	2.0
19 - 1st Dose	1.04	3.49	59.5	14.0
19 - 2nd Dose	0.48	2.47	58.5	12.0

The decrease in viable cells was then followed by a relatively steady regrowth until returning to the initial cell numbers approximately 3 days after the biocide treatment. The regrowth rates for experiments 3 and 4 were 0.105 hr^{-1} and 0.098 hr^{-1}, respectively. Table 5 gives the regrowth rates of the viable cells for all experiments.

Table 5. Biofilm regrowth rates after monochloramine treatment.

Experiment #	Regrowth Rate, hr^{-1}
3	0.105
4	0.098
10	0.211
12	0.120
14	0.102
17 - 1st Dose	0.089
17 - 2nd Dose	0.065
18 - 1st Dose	Not able to calculate
18 - 2nd Dose	0.046
19 - 1st Dose	0.080
19 - 2nd Dose	0.113
Average	0.103 ± 0.014

The total cell counts in experiments #3 and #4 only showed a 1 to 2 log decrease. The maximum decrease for the total cells was seen 30 to 40 hrs after the monochloramine was added to the system, much later than for viable cells.

A change in the dosing protocol showed a definite change in the reduction of viable and total cells numbers with time. Figure 5 shows the viable and total cell counts with time for experiment #10. A 2 mg L^{-1}, 4 hr monochloramine dose was added to the system in this experiment. The reduction in cell numbers was only 0.45 cfu m^{-2} for viable cells and 0.26 cells m^{-2} for total cells. This was not even a quarter of the reduction attained with the 4 mg L^{-1}, 2 hr dose even though it

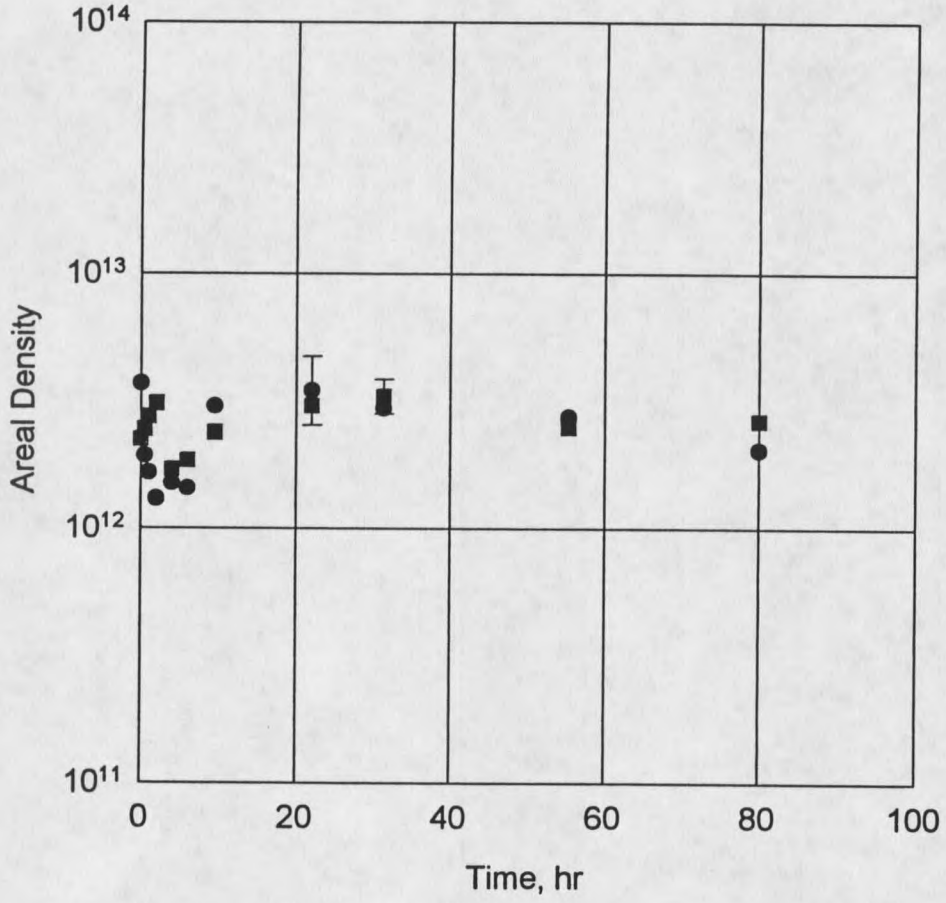

Figure 5. Experiment #10: 7-day old *Pseudomonas aeruginosa* biofilm treated with 2 mg L^{-1} monochloramine for 4 hr. Viable cell, cfu m^{-2}, (●) and total cell, cells m^{-2}, (■) areal densities vs. time. Error bars are shown on two points to indicate the statistical reliability of the plotted means. The viable cell error bar represents the SEM for 2 dilutions. The total cell error bar represents the SEM for 10 fields counted.

involved the same amount of biocide. Figure 6 presents a similar result for experiment #12. This experiment had a 2 mg L^{-1}, 8 hr monochloramine dose, twice the amount of biocide in experiments #3 and #4. Less than a quarter of the log reduction was again seen when compared to the 4 mg L^{-1}, 2 hr dose experiments. The time it took to attain the minimum for total cells was less than that for viable cells for this experiment. The regrowth rate for the viable cells was 0.120 hr^{-1}. This was similar to the regrowth rate seen for the 4 mg L^{-1}, 2 hr dose experiments.

Double dose experiments in which two monochloramine doses were administered at varied concentration and dose durations were performed. The viable and total cell reduction seen after each dose are presented separately. Figure 7 shows the viable and total cell number reduction for experiment #17. This double dose experiment consisted of 2 - 4 mg L^{-1}, 2 hr doses administered 40 hrs apart. Figure 7 shows a nearly 4 log reduction in viable cells after the first dose. The reduction of viable cells after the second dose was less. There was just a 1.65 log reduction after the second 4 mg L^{-1}, 2 hr dose was added to the system. The drop in total cells was similar after each dose. The drop was less than 1 log and occurred approximately 39.5 hr and 63.5 hr after the first and second doses, respectively. The regrowth rate of viable cells after the second dose was slower than the regrowth seen after the first dose, 0.065 hr^{-1} compared to 0.089 hr^{-1}. Figure 8 shows the results from another double dose experiment, experiment #18. This experiment consisted of a 2 mg L^{-1}, 4 hr dose added to the

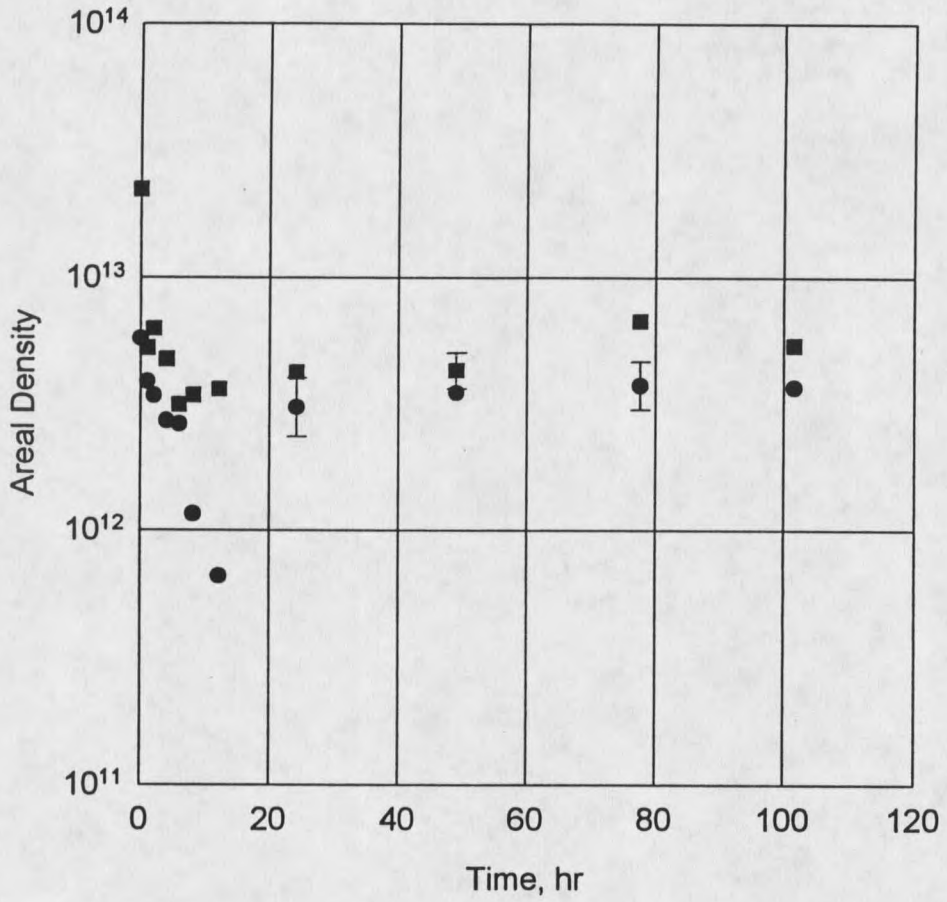

Figure 6. Experiment #12: 7-day old *Pseudomonas aeruginosa* biofilm treated with 2 mg L^{-1} monochloramine for 8 hr. Viable cell, cfu m^{-2}, (●) and total cell, cells m^{-2}, (■) areal densities vs. time. Error bars are shown on three points to indicate the statistical reliability of the plotted means. The first error bar on a viable cell point represents the SEM for 2 dilutions. The second error bar on a viable cell point represents the SEM for 3 dilutions. The total cell error bar represents the SEM for 10 fields counted.

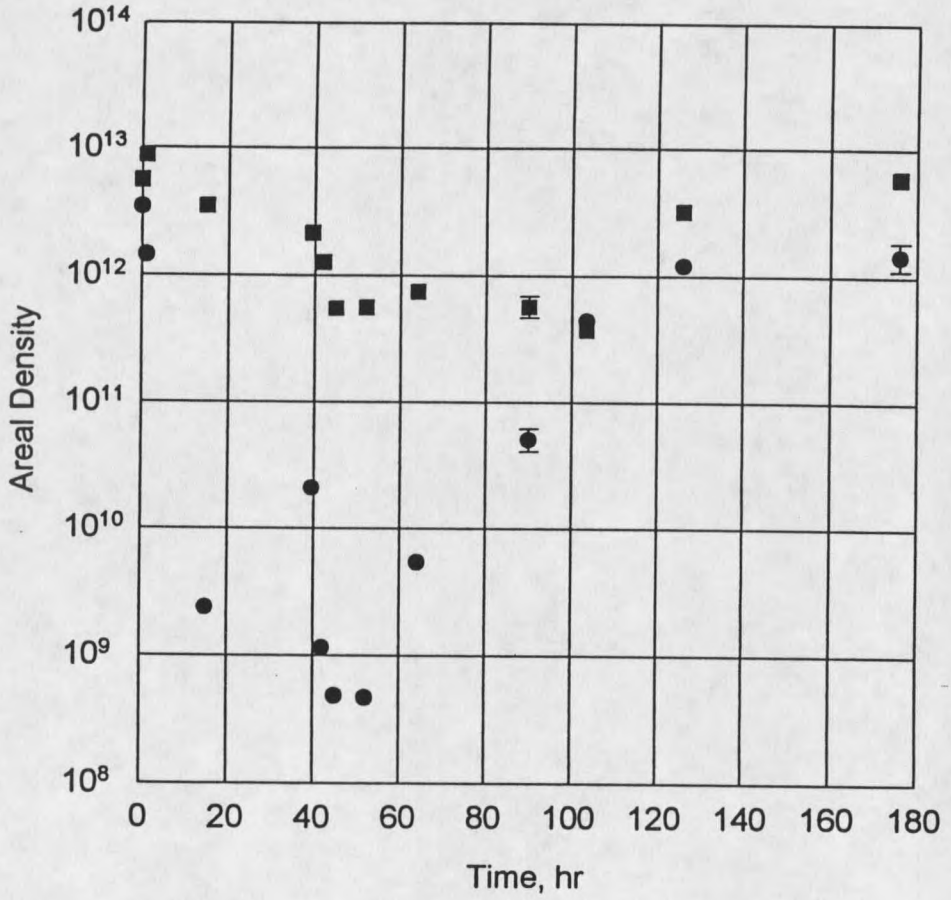

Figure 7. Experiment #17: Double dose experiment. 7-day old *Pseudomonas aeruginosa* biofilm treated with 2 monochloramine doses 40 hrs apart. Viable cell, cfu m^{-2}, (●) and total cell, cells m^{-2}, (■) areal densities vs. time. The first dose consisted of 4 mg L^{-1} monochloramine for 2 hr. The second dose consisted of 4 mg L^{-1} monochloramine for 2 hr. Error bars are shown on three points to indicate the statistical reliability of the plotted means. The first error bar on a viable cell point represents the SEM for 2 dilutions. The second error bar on a viable cell point represents the SEM for 3 dilutions. The total cell error bar represents the SEM for 10 fields counted.

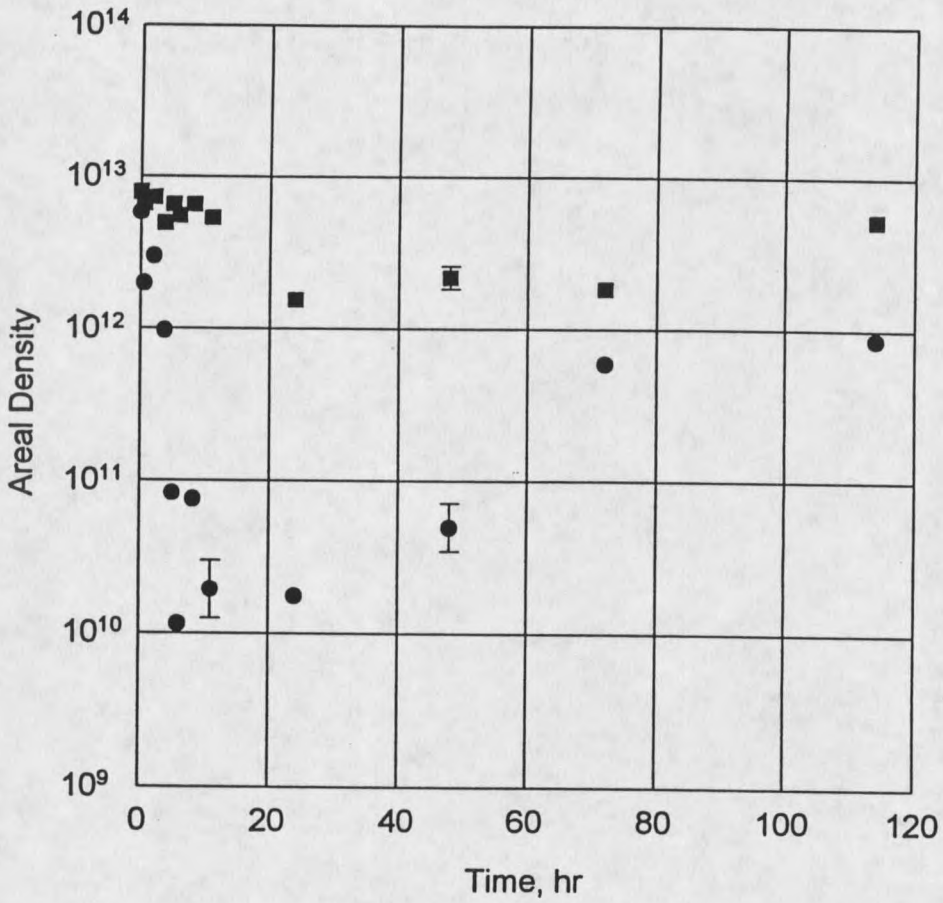

Figure 8. Experiment #18: Double dose experiment. 7-day old *Pseudomonas aeruginosa* biofilm treated with 2 monochloramine doses with no intermediate period. Viable cell, cfu m^{-2}, (●) and total cell, cells m^{-2}, (■) areal densities vs. time. The first dose consisted of 2 mg L^{-1} monochloramine for 4 hr. The second dose consisted of 4 mg L^{-1} monochloramine for 2 hr. Error bars are shown on three points to indicate the statistical reliability of the plotted means. The first error bar on a viable cell point represents the SEM for 2 dilutions. The second error bar on a viable cell point represents the SEM for 3 dilutions. The total cell error bar represents the SEM for 10 fields counted.

system followed immediately by a 4 mg L^{-1}, 2 hr dose. There was a small but recognizable drop in viable cells after the first dose. This minimum was attained immediately before addition of the second dose. Thus, a regrowth rate could not be calculated. There was minimal reduction in total cells before addition of the second dose. An additional approximately 2 log drop in viable cells was seen with the addition of the second dose. Less than 1 log reduction of total cells was obtained. The regrowth seen for the viable cells was just 0.046 hr^{-1}. This is about half the recovery rate seen with a single 4 mg L^{-1}, 2 hr dose.

Effluent Total Chlorine

The effluent total chlorine was sampled for all experiments immediately before, during, and approximately 1 hr after the monochloramine dose was added. Figure 9 shows the effluent total chlorine concentration curve for experiment #4. Approximately 3.60 mg L^{-1} of total chlorine was detected in the effluent from the system. This maximum amount was seen 140 min after addition to the system. Table 6 gives the breakthrough points in terms of maximum concentrations and time of the maximum for all the experiments. The desired dose concentrations and durations are given for reference.

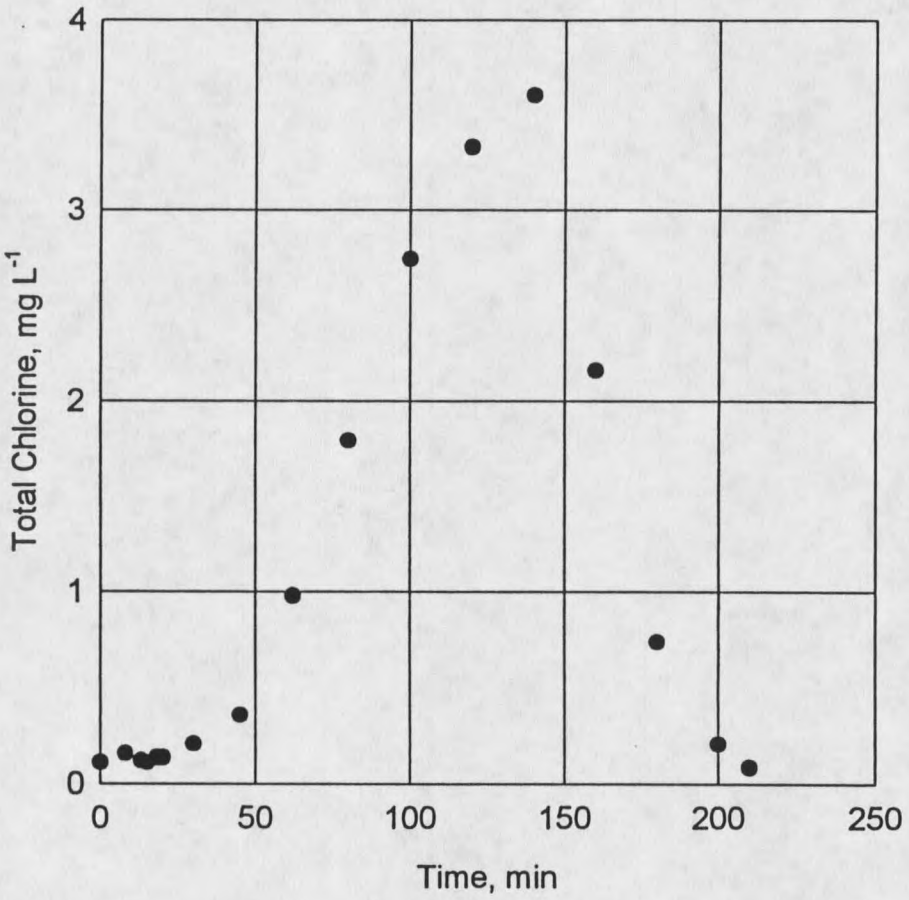

Figure 9. Experiment #4: Effluent total chlorine detected during 4 mg L^{-1}, 2 hr monochloramine dose. Total chlorine vs. time.

Table 6. Effluent total chlorine breakthrough points.

Experiment #	Dose Conc., mg L^{-1}	Dose Dur., hr	Maximum Conc., mg L^{-1}	Time of Maximum Conc., min
3	4	2	5.24	122
4	4	2	3.60	140
10	2	4	0.22	45
12	2	8	0.50	30
14	4	4	3.88	165
17 - 1st Dose	4	2	3.19	135
17 - 2nd Dose	4	2	3.24	120
18 - 1st Dose	2	4	0.37	20
18 - 2nd Dose	4	2	2.97	135
19 - 1st Dose	4	2	3.50	120
19 - 2nd Dose	4	2	4.24	120

Figure 10 shows the effluent total chlorine detected for experiment #12. Experiment #12 consisted of a single 2 mg L^{-1}, 8 hr dose. For this experiment, the maximum amount of chlorine detected was substantially less than what was added to the system. Only 0.5 mg L^{-1} was found in the effluent flow. This maximum was quickly obtained and continued to drop even as the monochloramine was still being added to the system.

Effluent total chlorine was similarly measured for the double dose experiments. The result for experiment #17 is shown in Figure 11. Very similar breakthrough curves are seen for the doses. The maxima were very close, 3.19 mg L^{-1} and 3.24 mg L^{-1}, for the first and second doses. Figure 12 shows the results for experiment #18. For this double dose experiment, duplicate effluent

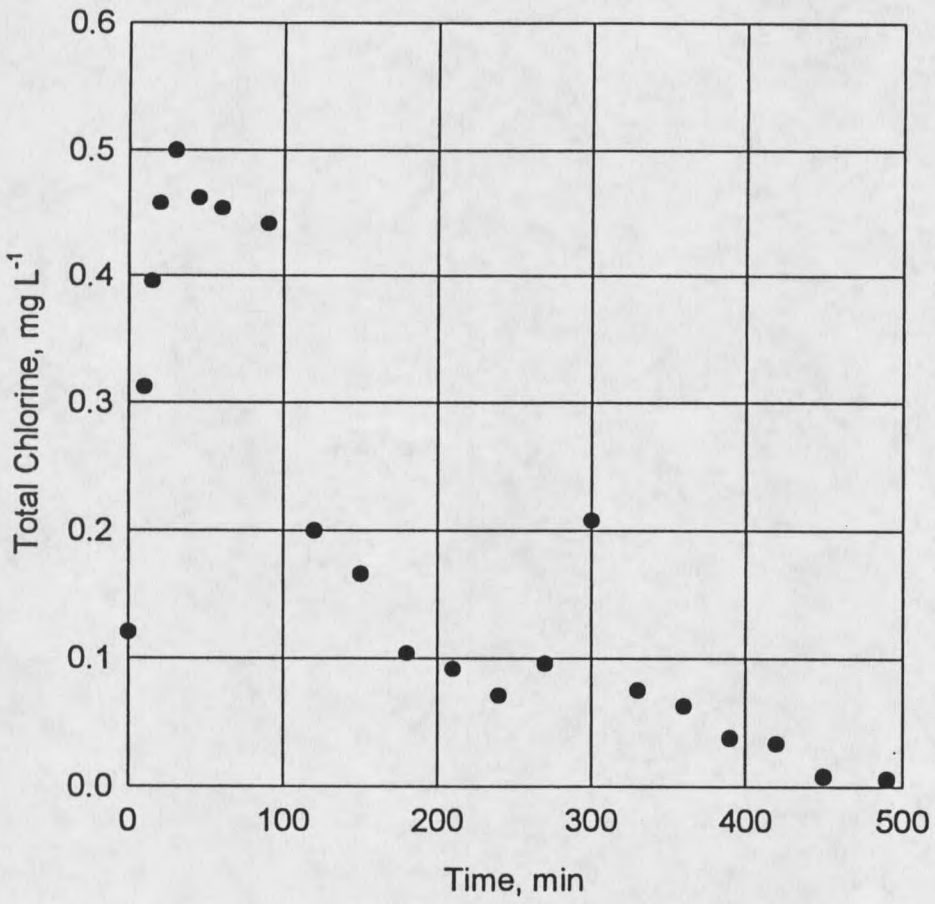

Figure 10. Experiment #12: Effluent total chlorine detected during 2 mg L^{-1}, 8 hr monochloramine dose. Total chlorine vs. time.

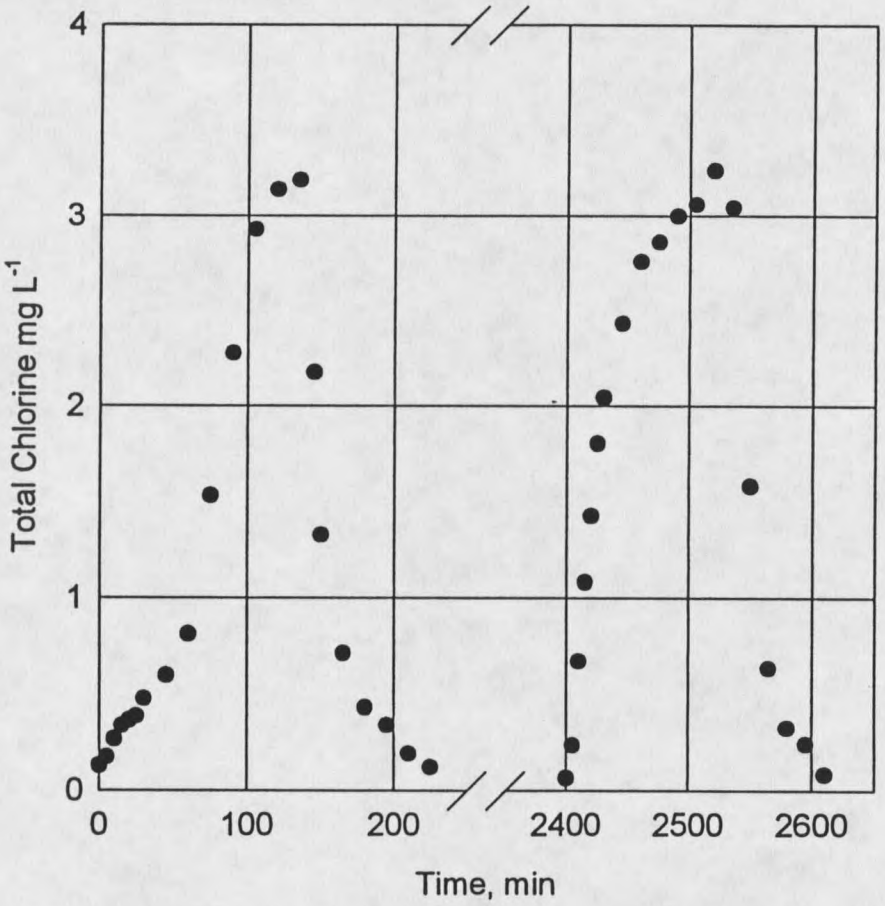

Figure 11. Experiment #17: Effluent total chlorine detected during 2 - 4 mg L^{-1}, 2 hr monochloramine doses added 40 hrs apart. Total chlorine vs. time.

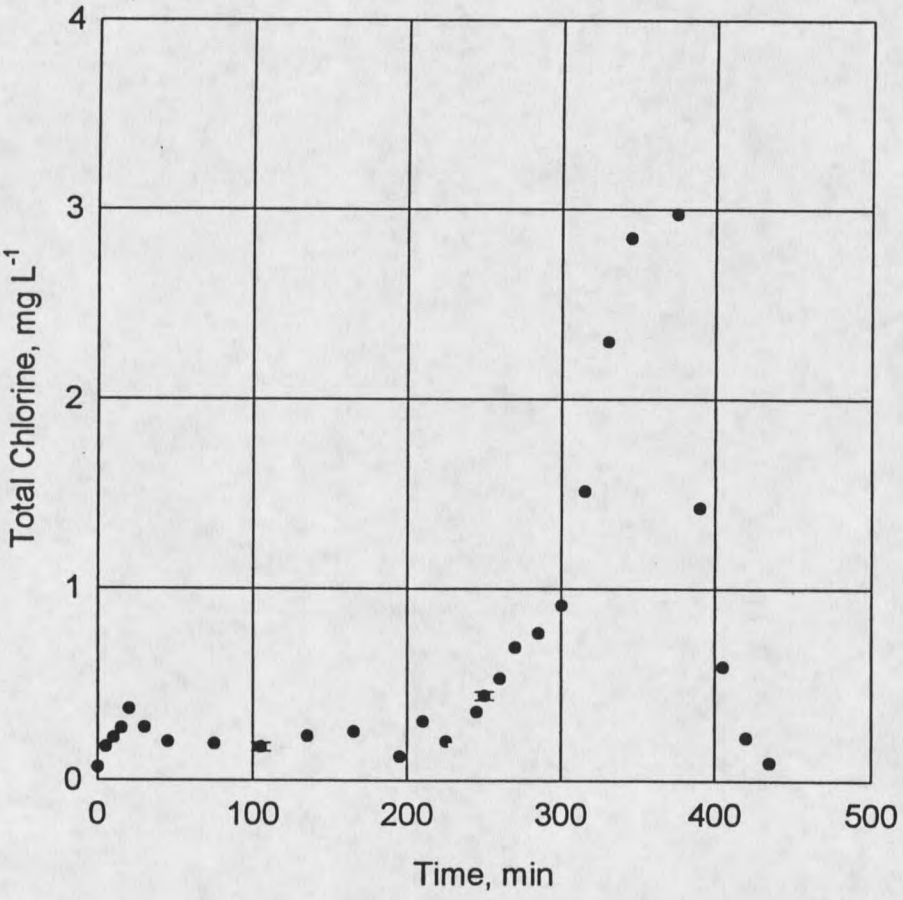

Figure 12. Experiment #18: Effluent total chlorine detected during a 2 mg L^{-1}, 4 hr monochloramine dose immediately followed by a 4 mg L^{-1}, 2 hr monochloramine dose. Total chlorine vs. time. Error bars represent the SEM for duplicate samples.

samples were taken. The SD for duplicates was small and the ± SEM error bars in Figure 12 are about the width of the plotted symbol. The effluent total chlorine measured for the initial dose was much less than what was added to the system. Its maximum was quickly seen before continuing to decrease. The second dose showed a maximum breakthrough of 2.97 mg L^{-1} approximately 135 min after being administered.

Reaction Rate

The reaction rate of monochloramine in the biofilm was examined as a function of time. Figure 13 shows the reaction rate of monochloramine in experiment #4. The effluent total chlorine concentration versus time was also plotted for reference. There is an initial high reaction rate that decreases with time until the end of the dose. During washout, the reaction rate remains at the low level. The change in reaction rate with time for experiment #12 is presented in Figure 14. The results seen in this experiment are essentially opposite of what was just described for experiment #4. In experiment #12, the reaction rate started low and continually increased until leveling out at around 200 min after the monochloramine dose was initiated. The reaction rate maintained nearly the same level through the rest of the dose until dropping to zero after the dosing period. The overall change in the reaction rate value, however, was actually very little. There was only a change of 0.03 mg min^{-1} from the initial level to the maintained maximum.

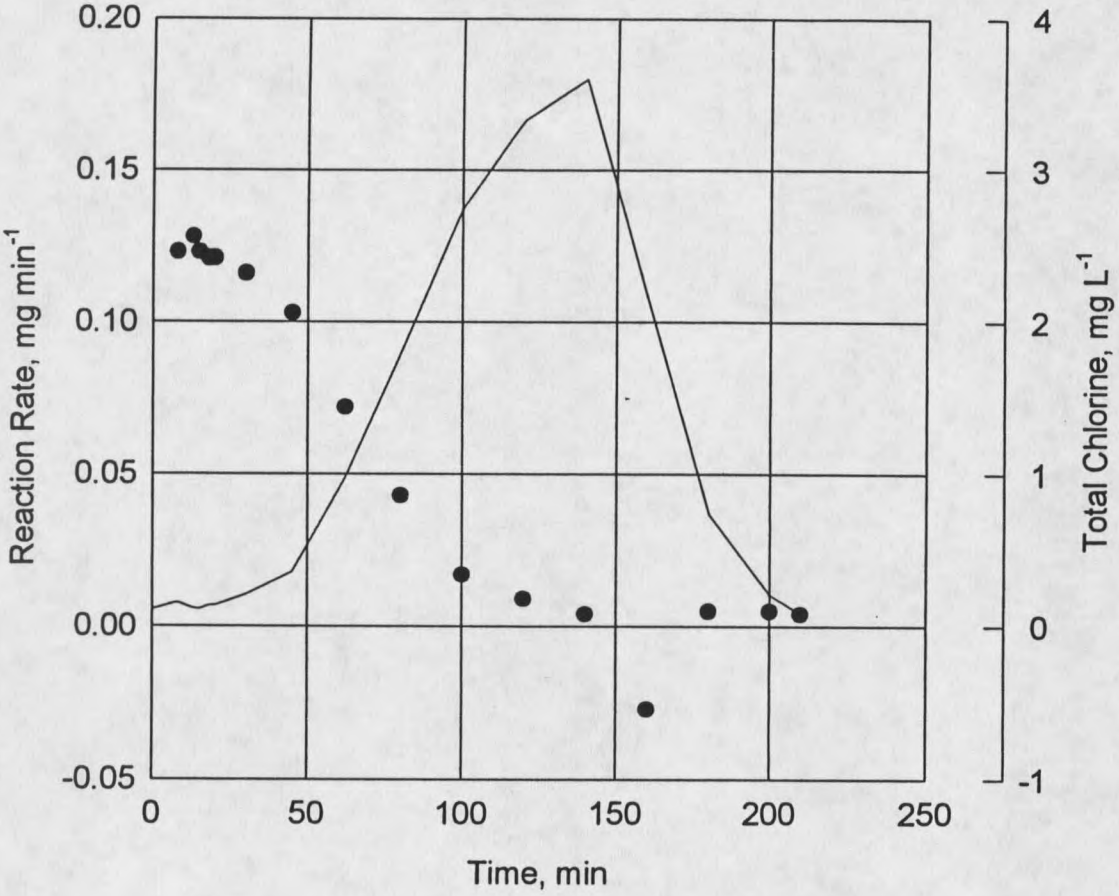

Figure 13. Experiment #4: Overall reaction rate of monochloramine with the biofilm during treatment. Reaction rate (●) vs. time. Total chlorine (—) vs. time.

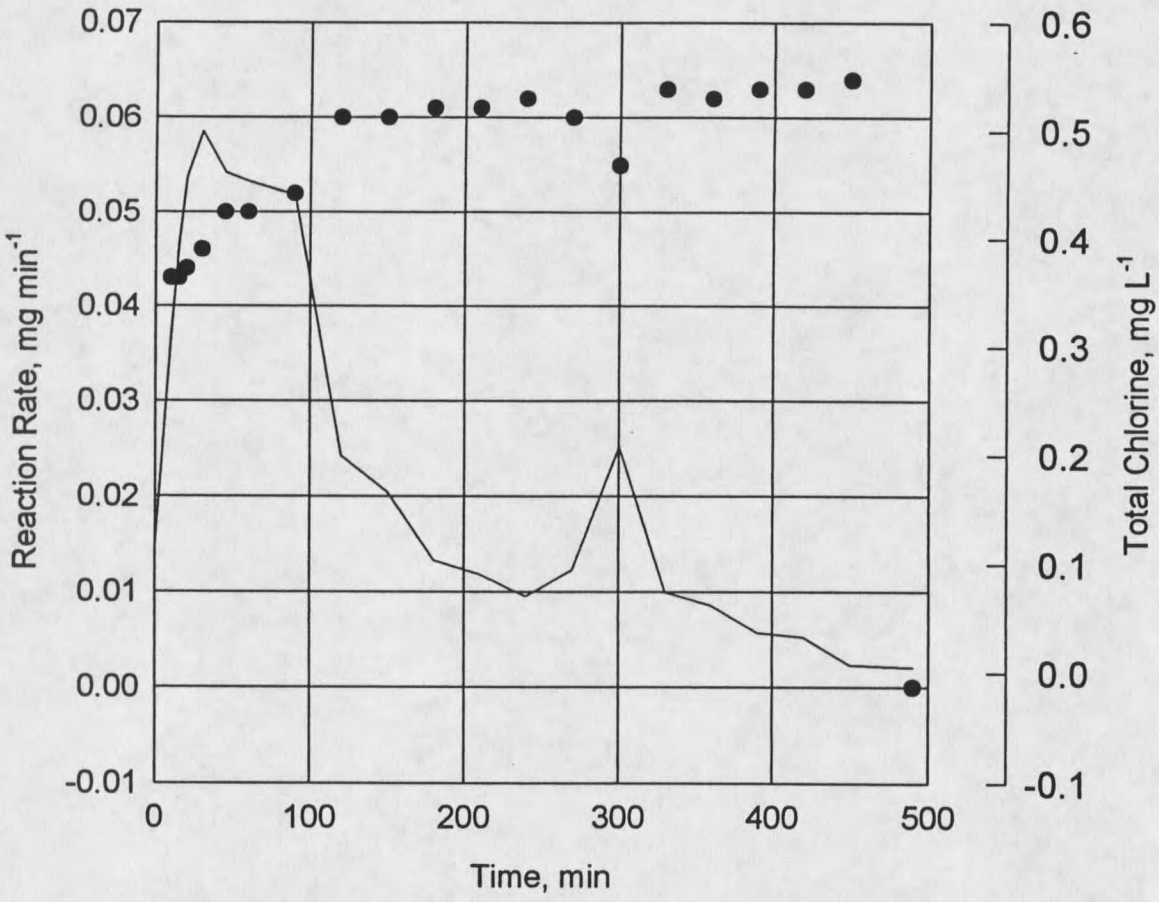

Figure 14. Experiment #12: Overall reaction rate of monochloramine with the biofilm during treatment. Reaction rate (●) vs. time. Total chlorine (—) vs. time.

Transport Limitation

Transport limitation of the monochloramine into the biofilm was analyzed by calculating observable moduli according to equation (25). Observable moduli were calculated at three points throughout the duration of the dose since the effluent concentration was continually changing. An observable modulus sufficiently large (greater than 3) means that there is transport limitation occurring (Bailey and Ollis, 1977). If the observable modulus is relatively small (less than 0.3), transport limitation does not dominate the system. Rather, chemical reaction would be the rate limiting process. In using this interpretation of the observable modulus, external mass transfer resistance is neglected. The three points at which observable moduli were calculated were approximately one quarter, one half, and three quarters of the dose duration. If the effluent total chlorine was not sampled at the exact interval, the next sampling time was used for calculation. Table 7 gives the observable modulus calculated at each point for all experiments. The average value was 0.381 ± 0.098. The maximum and minimum values were 2.415 and 0.000, respectively.

Table 7. Observable modulus for monochloramine in the biofilm.

Experiment #	Time, min	Φ		Experiment #	Time, min	Φ
3	34	0.478		17 - 1st Dose	30	0.356
3	60	0.010		17 - 1st Dose	60	0.165
3	100	0.000		17 - 1st Dose	90	0.019
4	30	0.898		17 - 2nd Dose	30	0.032
4	62	0.118		17 - 2nd Dose	60	0.018
4	100	0.010		17 - 2nd Dose	90	0.015
10	60	0.621		18 - 1st Dose	75	0.489
10	120	2.415		18 - 1st Dose	135	0.394
10	180	1.263		18 - 1st Dose	195	0.747
12	120	0.483		18 - 2nd Dose	30	0.229
12	240	1.406		18 - 2nd Dose	60	0.148
12	360	1.584		18 - 2nd Dose	90	0.020
14	60	0.004		19 - 1st Dose	30	0.359
14	135	0.004		19 - 1st Dose	60	0.215
14	180	0.006		19 - 1st Dose	90	0.024
				19 - 2nd Dose	30	0.019
				19 - 2nd Dose	60	0.015
				19 - 2nd Dose	90	0.002

Mathematical Model Studies

Modeling simulations were performed using AQUASIM for all experiments. The model was set to match the experimental conditions. The parameter estimation tool in AQUASIM was used for fitting the model to the experimental data. Table 8 contains the parameters and their values used for the simulations.

Table 8. Parameter values used for model simulation of experiments.

Parameter	Symbol	Value	Source
Volumetric flow rate	Q	1.92e-3 m^3 hr^{-1}	Project
Reactor bulk liquid volume	V	5.96e-4 m^3	Project
Biofilm surface area	A	0.184 m^2	[a, b]
Glucose concentration	S	20 g m^{-3}	Project
Monochloramine concentration	B	2 or 4 g m^{-3}	Project
Monochloramine dose duration	t_b	2, 4, or 8 hr	Project
Glucose diffusivity	D_s	2.484e-6 m^2 hr^{-1}	[c, d]
Monochloramine diffusivity	D_b	5.98e-6 m^2 hr^{-1}	[c, d]
Biofilm-bulk diffusivity ratio	T	0.9	[d]
Cell volume fraction	x_A	0.096	[e, f]
Cell intrinsic density	ρ_x	4.45e+4 g m^{-3}	[b]
Volume fraction neutralizer	N	0.004 g m^{-3}	Estimation
Neutralizer density	ρ_N	5.0e+3 g m^{-3}	Estimation
Maximum specific growth rate	μ_{MAX}	0.3 hr^{-1}	[g]
Yield coefficient for growth	Y_{xs}	0.34 g g^{-1}	[h]
Monod coefficient	K_s	2.0 g m^{-3}	[h]
Initial biofilm thickness	L_f	3.0e-5 m	[i, j]
Concentration boundary layer	L_L	1e-5 m	[k]
Detachment rate coefficient	k_d	m^{-1} hr^{-1}	Project
Yield coefficient for neutralizer	Y_{bn}	g g^{-1}	Fit
Monochloramine disinfection	k_{dis}	m^3 g^{-1} hr^{-1}	Fit
Monochloramine reaction rate	k_{rxn}	m^3 g^{-1} hr^{-1}	Fit

[a] Gjaltema *et al.*, 1994
[b] Peyton, 1992
[c] Perry *et al.*, 1984
[d] Westrin and Axelsson, 1991
[e] Drury, 1992
[f] Chen *et al.*, 1993
[g] Characklis, 1990(a)
[h] Robinson *et al.*, 1984
[i] Murga *et al.*, 1995
[j] Stewart *et al.*, 1993
[k] Christensen and Characklis, 1990

Certain parameters were fit for each experimental data set during the simulations. The final estimations for the fit parameters are presented in Table 9.

Table 9. Fit parameter values used for model simulation of experiments.

Experiment #	k_{rxn}, $m^3\ g^{-1}\ hr^{-1}$	k_{dis}, $m^3\ g^{-1}\ hr^{-1}$	Y_{bn}, $g\ g^{-1}$
3	100	1.95	4.50
4	100	1.95	4.50
10	29.0	2.00	35.0
12	27.0	1.70	35.0
14	200	0.90	2.00
17 - 1st Dose	100	1.95	4.50
17 - 2nd Dose	50.0	1.70	8.00
18 - 1st Dose	29.0	2.00	35.0
18 - 2nd Dose	40.0	1.40	7.00
19 - 1st Dose	100	1.95	4.50
19 - 2nd Dose	50.0	1.50	6.00

As seen in Table 9, the doses in the double dose experiments were treated separately. The reason for this will be explained later in this section.

Viable and Total Cells

The viable and total cell data from each experiment was imported into AQUASIM. The initial conditions were then set and the parameter estimation performed. All of the following figures will consist of both the model fits and experimental results so that evaluation will be easier. The model fit for

experiment #4 is presented in Figure 15. The model fit was able to capture approximately the same drop in viable cells followed by a steady regrowth back to the original number. This regrowth was faster than what was seen experimentally. There is also a drop in total cells. This drop was only around 0.5 to 1 log, which was a little less that what was experimentally observed. The minimum total cell number was reached around 27.8 hrs before quickly returning to the initial level. The model fit did pick up the trends seen in the experimental system. A model fit was made for experiment #12. This result is presented in Figure 16. The model again readily gives the drop in viable cells and a steady regrowth. The total cells dip slightly and rapidly return to the original level.

By looking at the various fit parameters in Table 9, it is seen that they can be up to an order of magnitude different for 2 of the 3 parameters. This order of magnitude difference even occurs when the same overall amount of monochloramine is being added to the system through different protocol. Experiment #4 and experiment #10 both involved adding the same amount of biocide to the system, just by different protocols. The parameters used for making these fits were found to be very different. A problem then arises in attempting to use one set of parameters for fitting both experiments. Figures 17 and 18 demonstrate these problems. Figure 17 shows the model prediction for experiment #4 using the parameter values fit to experiment #10. With these parameters, the model can not accurately predict the reduction and regrowth of viable or total cells. A similar result is seen in Figure 18. This figure gives the

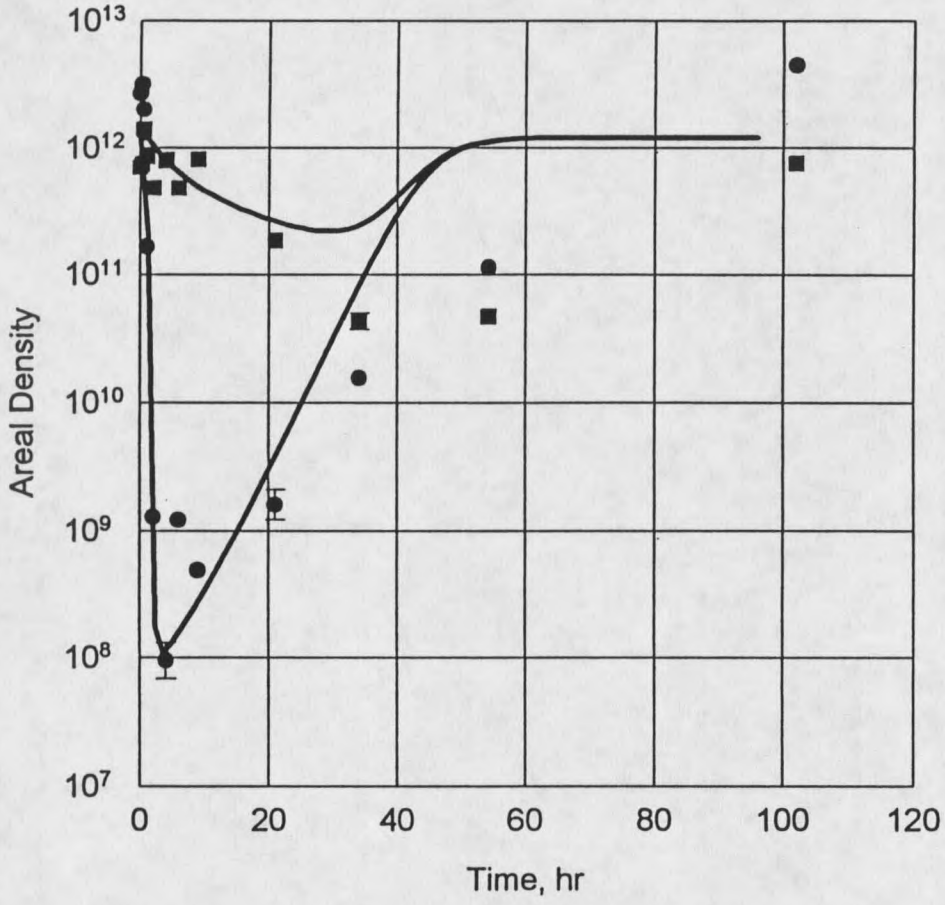

Figure 15. Model simulation for experiment #4 using AQUASIM. Model fit viable cell, cfu m^{-2}, and total cell, cells m^{-2}, areal densities (—) vs. time. Experimental viable cell, cfu m^{-2}, (●) and total cell, cells m^{-2}, (■) areal densities vs. time.

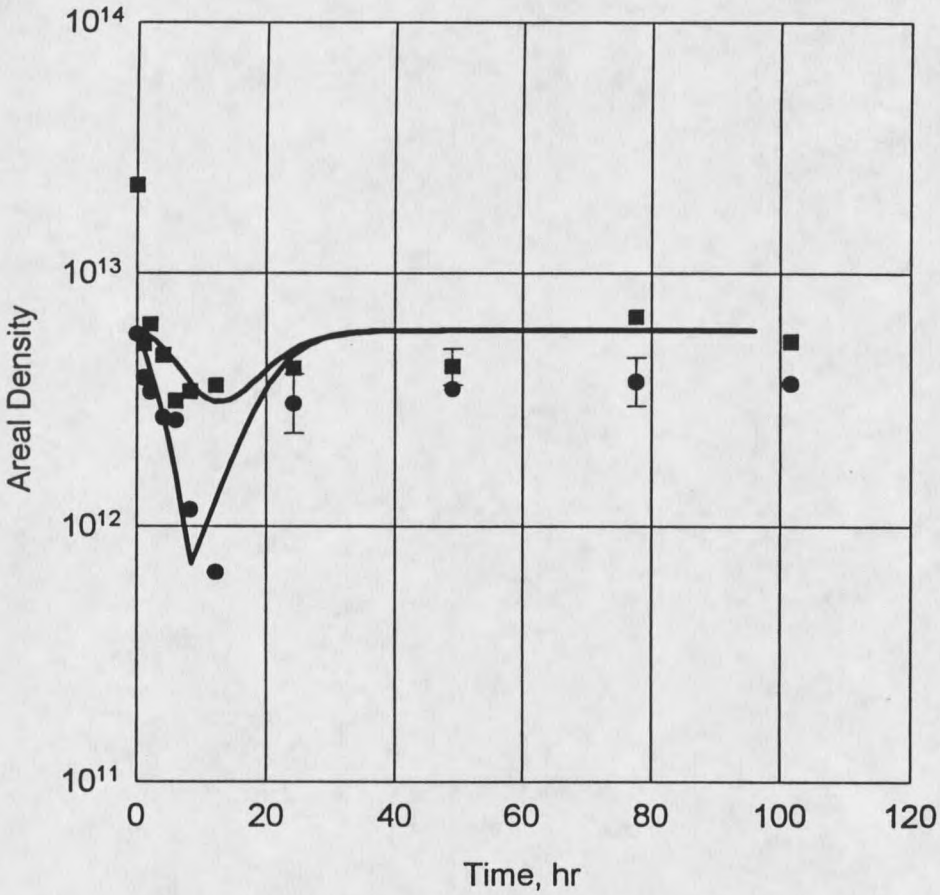

Figure 16. Model simulation for experiment #12 using AQUASIM. Model fit viable cell, cfu m^{-2}, and total cell, cells m^{-2}, areal densities (—) vs. time. Experimental viable cell, cfu m^{-2}, (●) and total cell, cells m^{-2}, (■) areal densities vs. time.

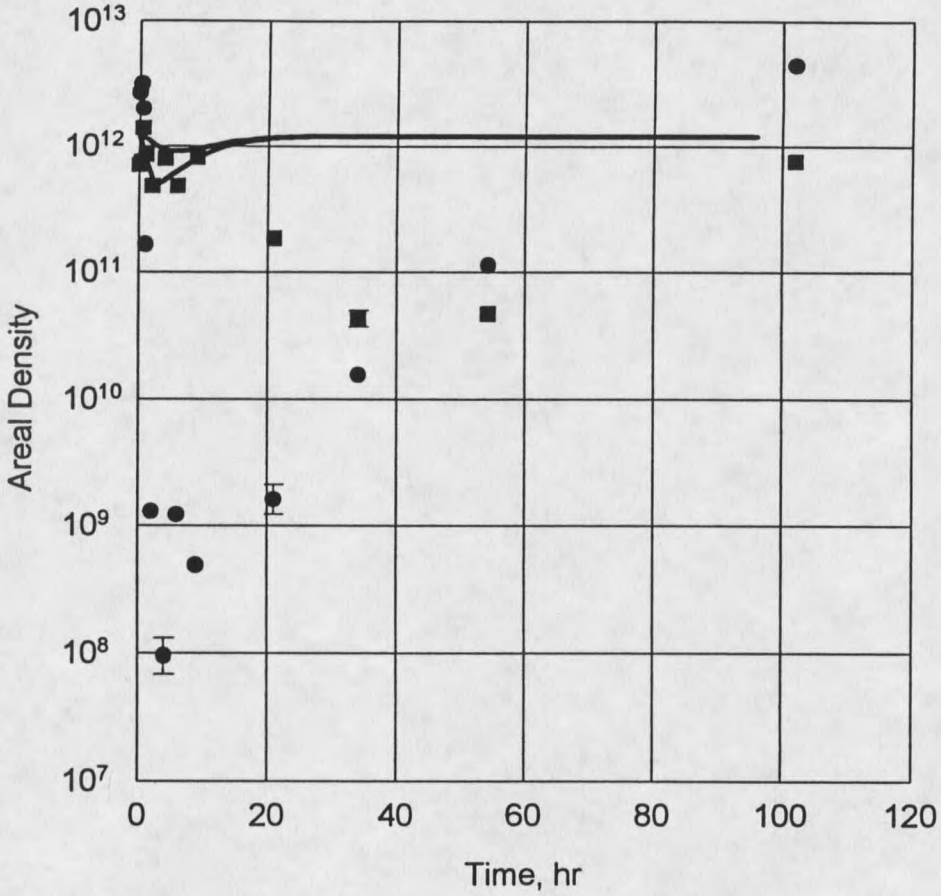

Figure 17. Model simulation for experiment #4 using fit parameters for experiment #10. Model predicted viable cell, cfu m^{-2}, and total cell, cells m^{-2}, areal densities (—) vs. time. Experimental viable cell, cfu m^{-2}, (●) and total cell, cells m^{-2}, (■) areal densities vs. time.

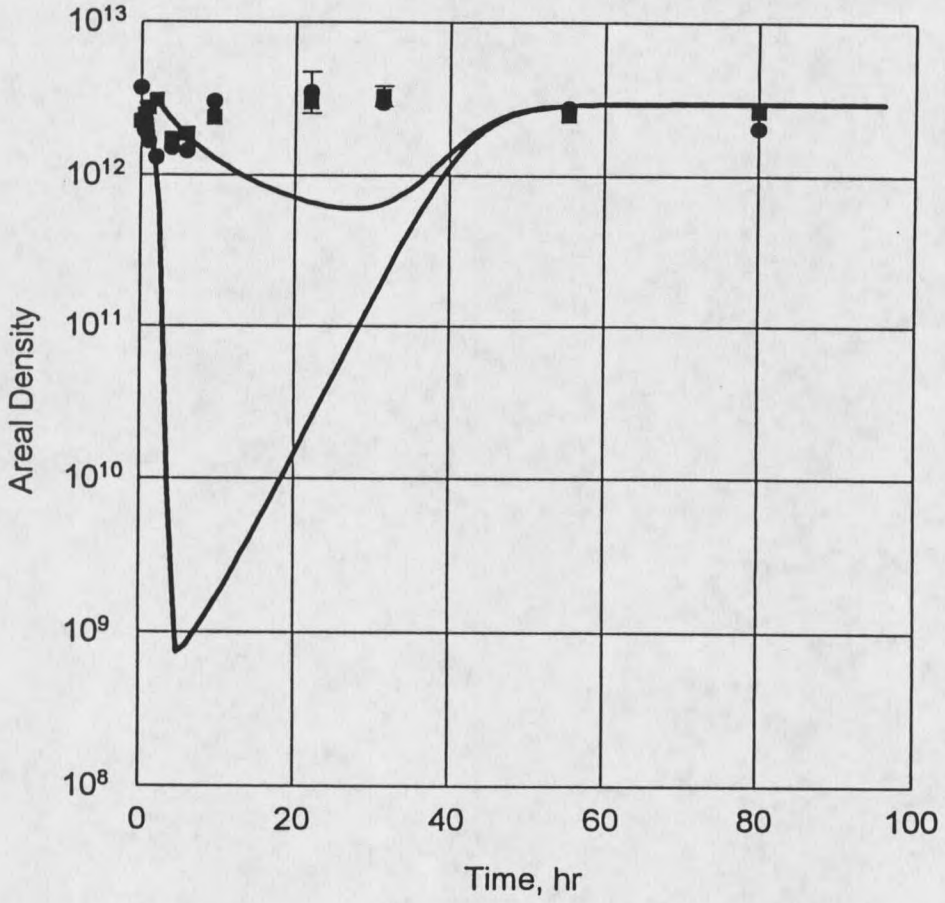

Figure 18. Model simulation for experiment #10 using fit parameters for experiment #4. Model predicted viable cell, cfu m^{-2}, and total cell, cells m^{-2}, areal densities (—) vs. time. Experimental viable cell, cfu m^{-2}, (●) and total cell, cells m^{-2}, (■) areal densities vs. time.

prediction of experiment #10 using parameters from experiment #4. There is a much greater reduction in viable and total cells predicted than what was seen experimentally.

Similar problems appeared when simulating double dose experiments in that the parameter values set for the first dose did not readily fit the results seen after the second dose. Figure 19 shows the model prediction for experiment #17, where the second dose was 40 hrs after the initial dose. This model prediction was made preceding the experimental work. This figure shows that the model predicted a greater reduction in viable cells than was seen experimentally. The model predicted nearly a 6 log reduction after the second dose, while only around a 2 log drop was seen. The total cell drop was relatively close. There is a somewhat hidden problem in this prediction, however. Experimentally the second dose was administered when the total cells were at their lowest values, at 40 hrs. In the model prediction, the total cells were not at their lowest point at 40 hrs. They were already in the regrowth stage at this time. The total cell minimum in the model prediction came at 27.8 hrs after the dose. Figure 20 shows the results for the prediction when having the model implement the second dose at the time of its minimum cell number. There was again a 6 log drop shown after the second dose. The minimum value of viable cells, however, was less than previously seen. Figures 19 and 20 showed the need to divide the prediction into two parts and estimate parameters for the first and second doses separately. A better fit was obtained for the second dose when a

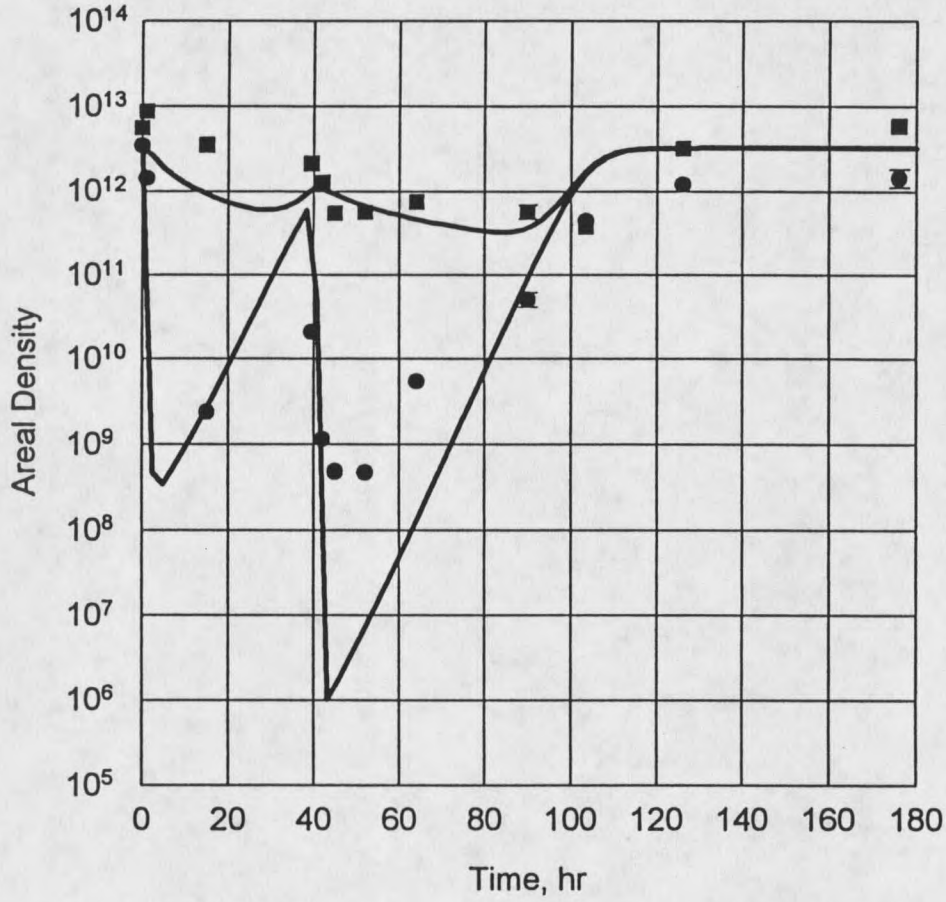

Figure 19. Model simulation for experiment #17 using AQUASIM. The model prediction second dose set for 40 hrs after first dose. Model prediction viable cell, cfu m^{-2}, and total cell, cells m^{-2}, areal densities (—) vs. time. Experimental viable cell, cfu m^{-2}, (●) and total cell, cells m^{-2}, (■) areal densities vs. time.

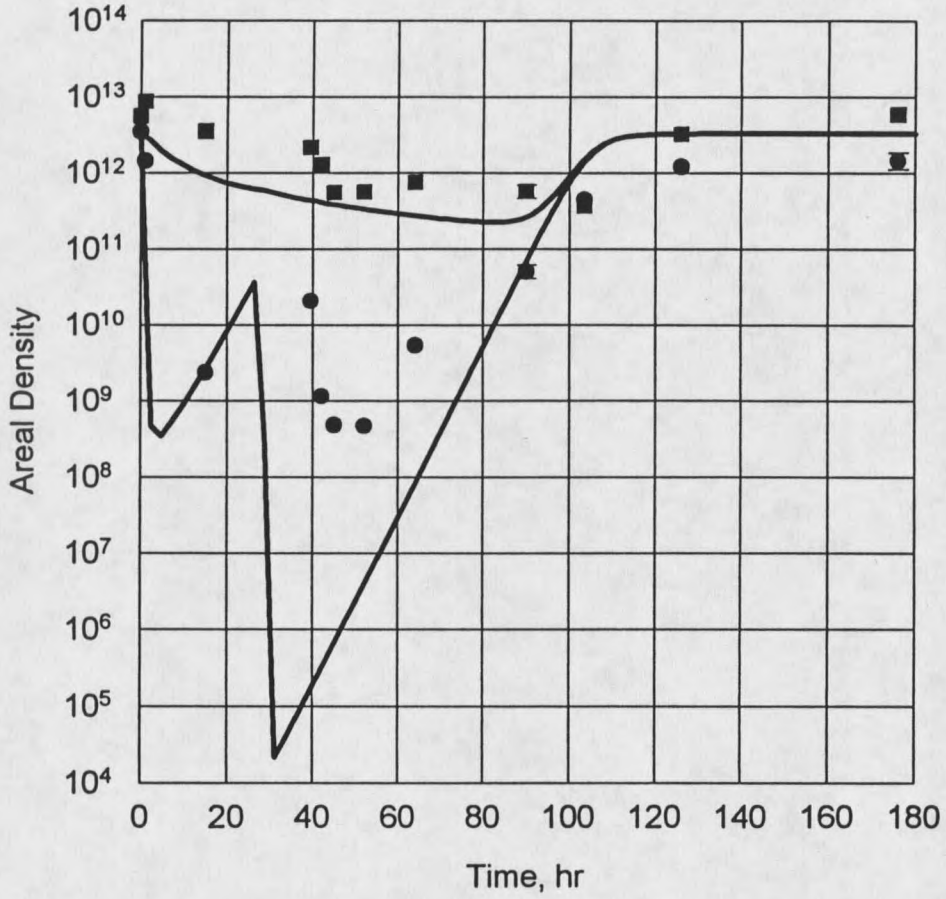

Figure 20. Model simulation for experiment #17 using AQUASIM. The model prediction second dose set for 27.8 hrs after first dose. Model prediction viable cell, cfu m^{-2}, and total cell, cells m^{-2}, areal densities (—) vs. time. Experimental viable cell, cfu m^{-2}, (●) and total cell, cells m^{-2}, (■) areal densities vs. time.

separate parameter estimation was performed.

Effluent Total Chlorine

The model was used to fit the breakthrough curves for monochloramine in the system. The fit breakthrough curve for experiment #4 is shown in Figure 21. This figure shows an initial small delay then a steady increase in concentration until reaching close to 4 mg L^{-1}. A short washout period followed. It was very similar to the experimental results. The model fit was able to capture the initial delay that was seen experimentally. The following increase in concentration was faster, but the same trends were seen.

A few problems arose when attempting to fit the results for experiments in which the monochloramine peaked early and then decreased in concentration over time (the 2 mg L^{-1} experiments). Figure 22 presents a model fit where this situation occurred. It is a fit for experiment #12. The best fit that was attained involved a very slow increase in concentration until peaking at a low concentration at the end of the dose. The fit appeared to be opposite of what was experimentally demonstrated.

The monochloramine breakthrough curves for the double dose experiments were also fit. Figure 23 presents the curves for experiment #17 using the same parameters for each dose. The shape of the curves was captured in each, although the concentration at breakthrough was greater than what was experimentally observed for both doses. The sharp increase in concentration

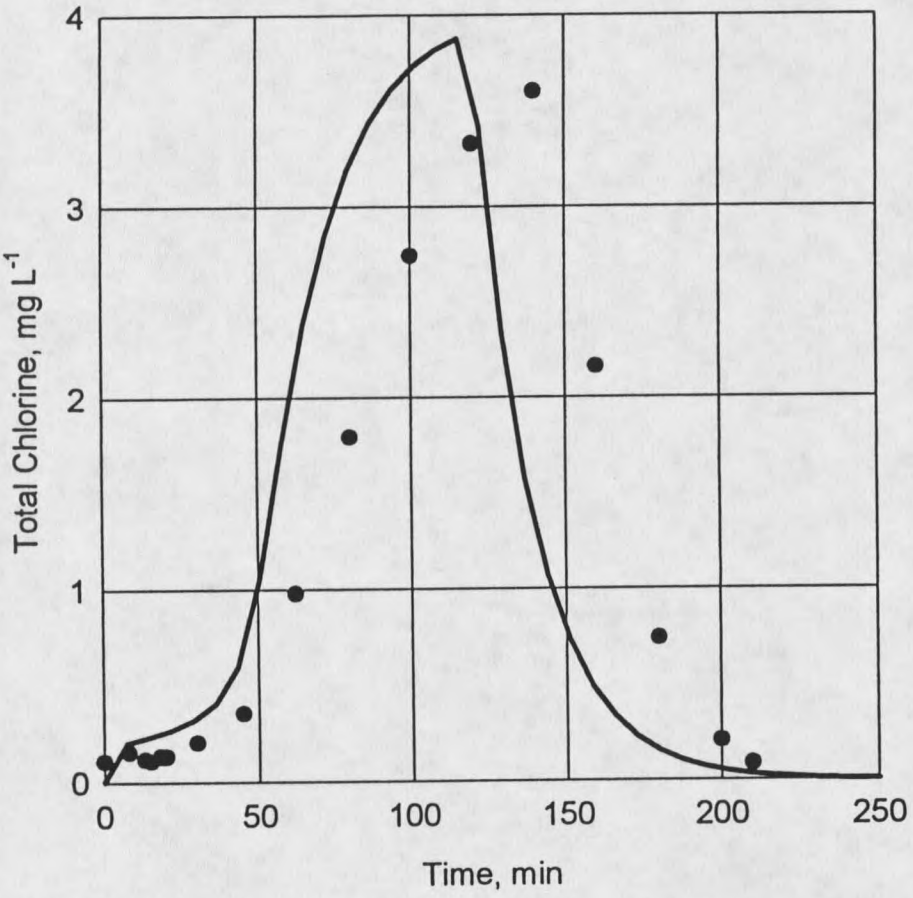

Figure 21. Model simulation for experiment #4 using AQUASIM. The model fit effluent total chlorine. Model fit total chlorine (—) vs. time. Experimental total chlorine (●) vs. time.

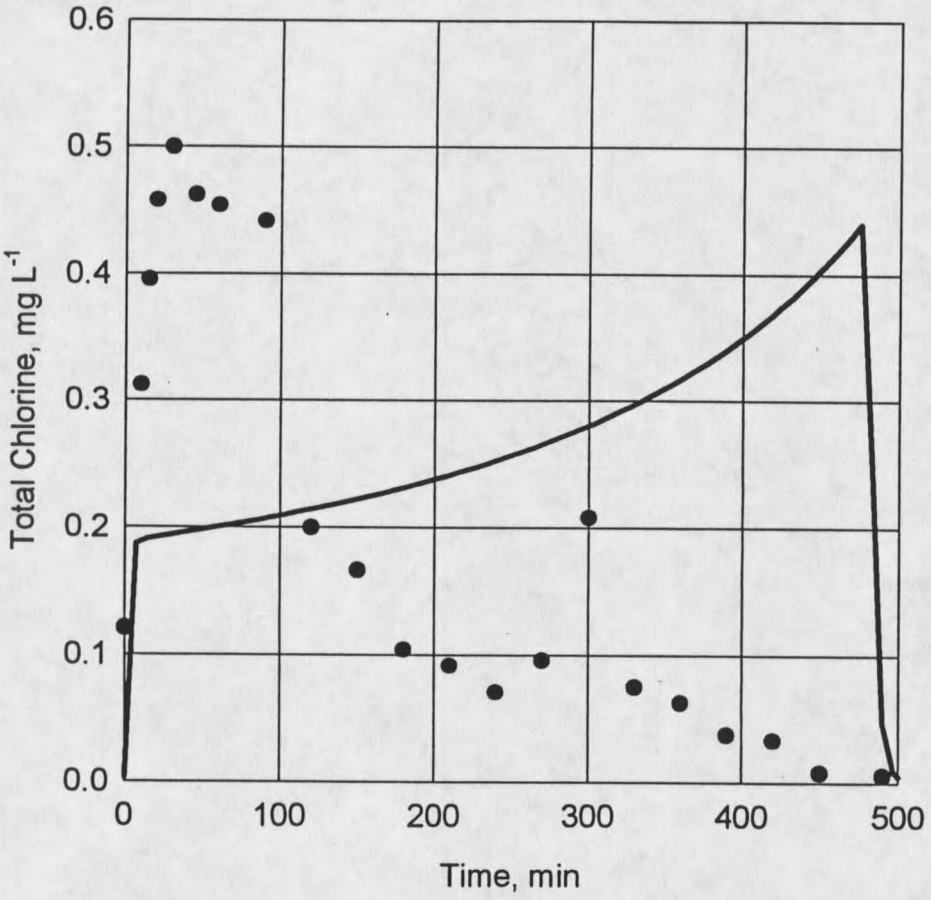

Figure 22. Model simulation for experiment #12 using AQUASIM. The model fit effluent total chlorine. Model fit total chlorine (—) vs. time. Experimental total chlorine (●) vs. time.

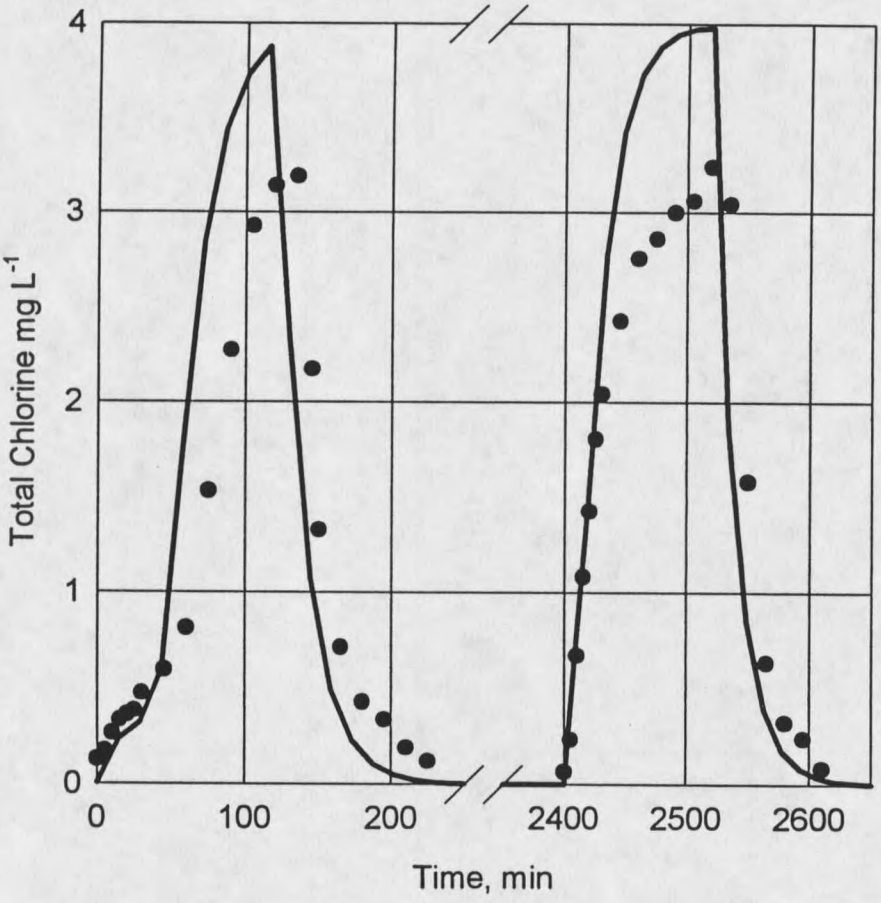

Figure 23. Model simulation for experiment #17 using AQUASIM. Model fit effluent total chlorine for 40 hrs between doses. Model fit total chlorine (—) vs. time. Experimental total chlorine (•) vs. time.

after initiation of the second dose was seen both experimentally and in the model fit.

Transport Limitation

The monochloramine gradients in the biofilm were predicted with AQUASIM. Figure 24 shows the gradients predicted for experiment #4. The gradients were predicted for every 0.5 hr interval during the dosing period. Very little limitation was seen in the prediction. There was essentially complete penetration of the monochloramine to the substratum at the bulk concentration levels, even at the high concentrations. A similar result is seen in Figure 25. Figure 25 shows the predicted gradients for experiment #12. The gradients were found at 1 hr intervals during the duration of the dose. The monochloramine was able to penetrate through the biofilm to the substratum at close to the initial concentration levels. There was a small reduction in concentration during penetration, but less than 0.05 mg L^{-1} or 11 percent for all cases.

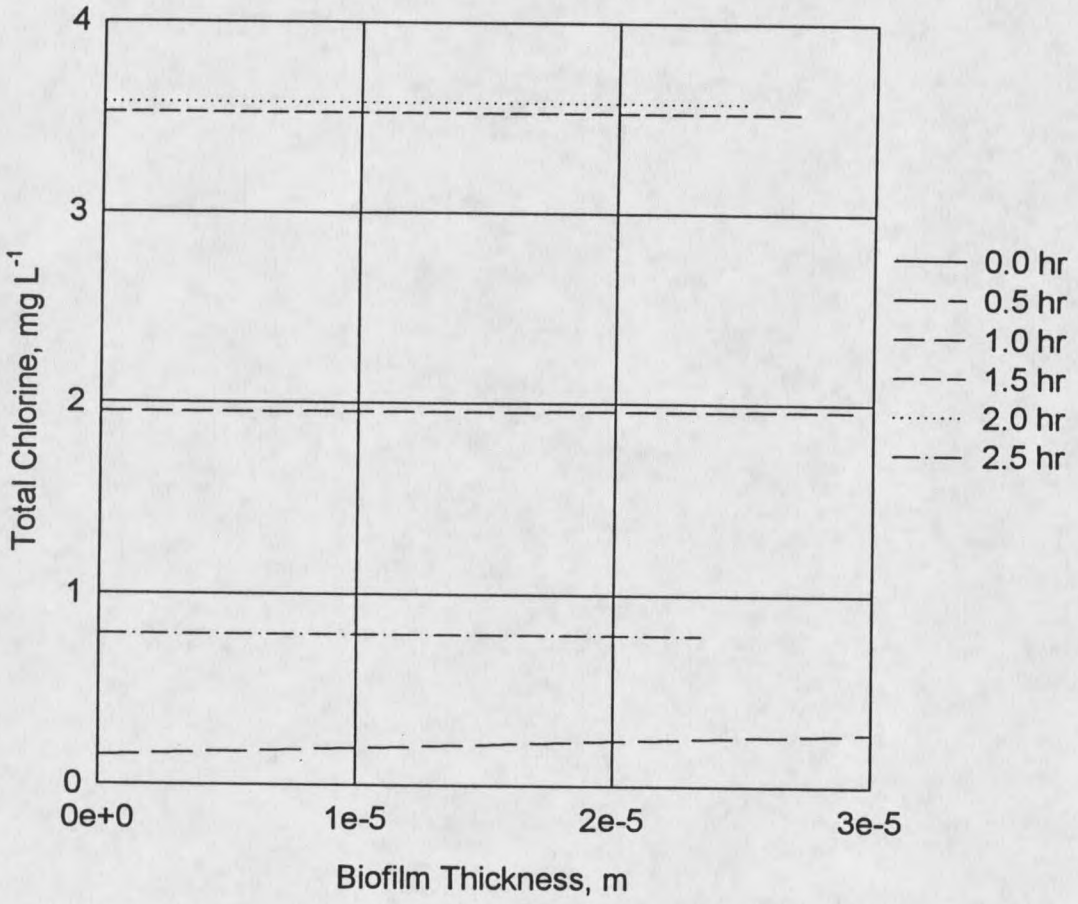

Figure 24. Model simulation for experiment #4 using AQUASIM. Model predicted monochloramine gradients with time. The substratum is at 0e+0 m. Model predicted total chlorine vs. biofilm thickness.

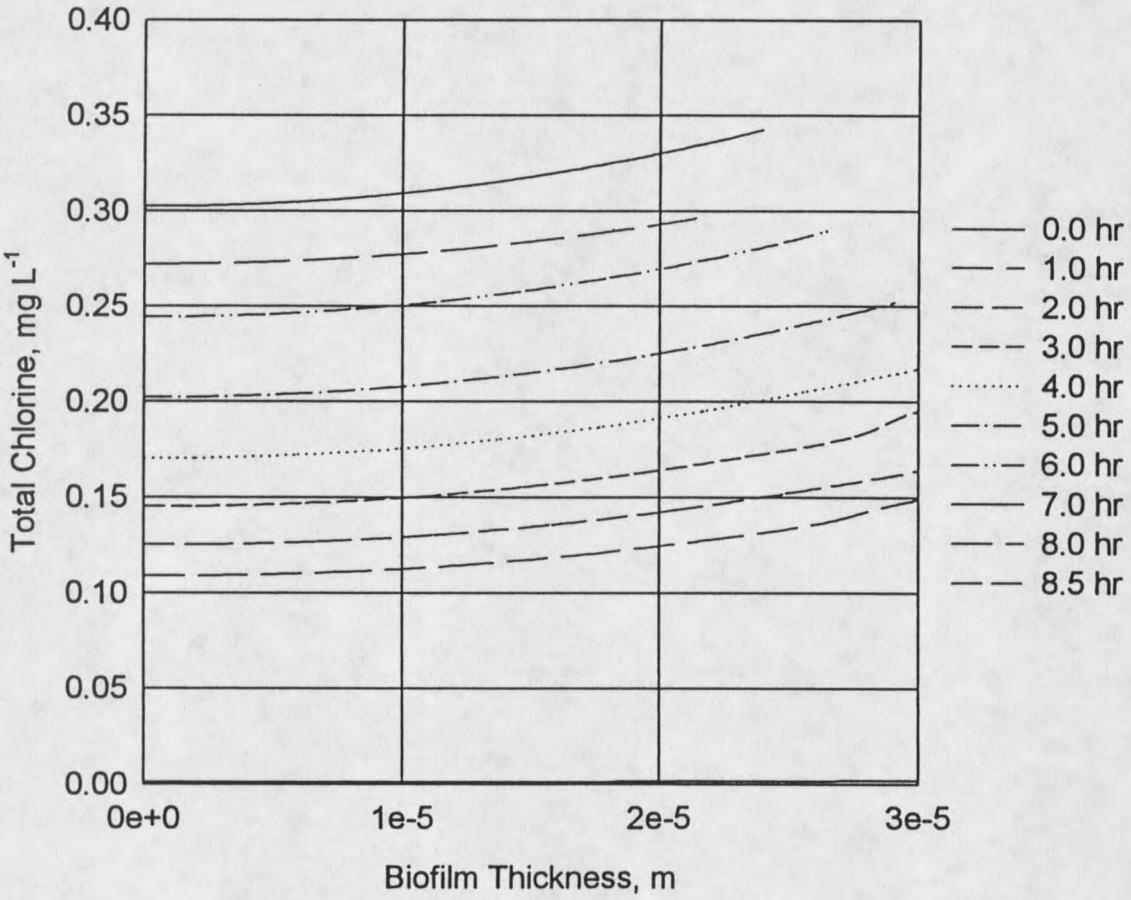

Figure 25. Model simulation for experiment #12 using AQUASIM. Model predicted monochloramine gradients with time. The substratum is at 0e+0 m. Model predicted total chlorine vs. biofilm thickness.

DISCUSSION

Annular Reactor Studies

Viable and Total Cells

Monochloramine caused transient reductions in viable and total cell numbers when applied to a *P. aeruginosa* biofilm. The extent of the reductions depended on the dosing protocol. When a lower dose of monochloramine, such as 2 mg L^{-1}, was added to the system very little reduction in the viable and total cells occurred. This was observed regardless of the length of the dose. The maximum reduction of viable cells seen with the lower (2 mg L^{-1}) dose experiments was 0.90 log. Total cells were reduced even less. These reductions can be compared to the drop in cells seen when a higher monochloramine dose, such as 4 mg L^{-1}, was added to the system. In duplicate 4 mg L^{-1}, 2 hr dose experiments, a 4 to 5 log reduction in viable cells was reproducibly seen. Extending this dose concentration to a duration of 4 hr further increased the reduction in viable cells to between 5 and 5.5 log. These results point toward the concentration, not the duration of the dose, being the more important variable in controlling biofilms. Characklis (1990(b)) found this same result of concentration being the deciding factor for the overall efffectiveness of the dose.

The dosing protocols were not only altered by changing the concentration

and duration of the dose, but also by adding a second dose during the experimental run. Three different experiments were performed in which an additional dose was administered. For these experiments, the first dose demonstrated a very similar effect on the viable and total cells as previously seen with doses of the same concentrations and durations. The effect of the second dose, however, was lessened. When a second dose with the same concentration and duration as the first dose was added 40 hrs after the first dose, the further reduction in viable cells was only about half of what was previously seen. This experiment was repeated with a time of 60 hrs between doses. The results from this experiment showed a little more reduction in viable cells after the second dose, but still less than two thirds as much as was seen with the first dose. A third double dose experiment involved a first dose administered at a low concentration followed immediately by a dose of higher concentration. The second dose did not show the same reduction in viable cells as was previously seen with the same dose concentration and duration.

Regrowth rates of the viable cells were very similar for the single dose experiments with the exception of the 2 mg L^{-1}, 4 hr dose experiment. The regrowth rate was 0.211 hr^{-1} for this experiment, compared to 0.105 hr^{-1}, 0.098 hr^{-1}, 0.120 hr^{-1}, and 0.102 hr^{-1} for the others. All of the regrowth rates were slower than the maximum growth rate of *P. aeruginosa* which has been found to be around 0.30 hr^{-1} (Characklis, 1990(a)). The regrowth rates were just a third of this maximum growth rate. The reason for this slower regrowth rate was not

investigated. One hypothesis for this slow regrowth was that there had been a physiological adaptation by the bacteria after being exposed to the monochloramine. In other words, the bacteria were responding to the monochloramine in their biofilm environment by altering their normal life cycle in the biofilm. Brözel *et al.* (1993) have shown that bacteria can become more resistant to repeated biocide doses by adaptation. The double dose experiments also support the idea of adaptation on the part of the biofilm to become less susceptible.

The regrowth rates of viable cells seen after the first dose of the double dose experiments were very similar to what had been previously seen in the single dose experiments. The regrowth rates after the second doses were somewhat slower in two of the three experiments. The rates were only two thirds to one half as fast in the experiment with 40 hrs between doses and the experiment with the immediate second dose. The experiment with 60 hrs between doses did not show a change in the regrowth rate. These reduced regrowth rates may also support a hypothesis of a physiological adaptation. This was not investigated further in this work.

Effluent Total Chlorine

The detection of total chlorine in the effluent implied that the biofilm system was not able to fully react with or consume all of the monochloramine available. There were two distinct trends seen in the effluent total chlorine data. The trend

observed for an experiment was determined by the concentration of the dose. The duration of the dose did not appear to readily affect the amount of total chlorine detected. One trend seen was a reproducible breakthrough curve peaking near the influent concentration at the end of the dose duration. The higher concentration (4 mg L^{-1}) doses showed this trend. The other trend seen was a low peak near the beginning of the dose followed by a continual decrease in effluent total chlorine throughout the remaining duration of the dose. The lower concentration (2 mg L^{-1}) dose experiments showed this trend. For these experiments, the maximum concentration was obtained around the first quarter of the dose duration. This maximum was at most a quarter of the influent concentration. The same trends were seen, in respect to the concentration of the dose, for the double dose experiments. The effluent total chlorine results again point toward a possible physiological adaptation by the bacteria. In the lower concentration dose experiments, an uncharacterized change occurred making the *P. aeruginosa* biofilm able to consume monochloramine more rapidly. This response was not further investigated.

Reaction Rate

The reaction rate of monochloramine with biofilm appeared to be controlled by the amount of reactive biomass available in the system. In looking at the reaction rate as a function of time, the higher concentration (4 mg L^{-1}) doses had reaction rates which started high and slowed down during the duration of the

dose. They stayed down during the washout period. These results point toward the conclusion of the reaction rate being controlled by the amount of reactive biomass available for the monochloramine. It appeared that reactive biomass was depleted during the dose. The reaction rate of lower concentration (2 mg L^{-1}) doses did not show this same behavior. The reaction rates in these experiments started low and increased during the first half of the dose. They then leveled off at this rate and remained steady during the rest of the dose. The overall change in the reaction rate, however, was just a fifth of the change seen during the higher dose experiments. The rates were also only one third to one half as fast as the reaction rates seen with the high doses. These lower rates mean the reactive constituent was being used up more slowly. There also appears to be an increase in the amount of reactive biomass available during the duration of the dose. If the reaction rate was controlled by the amount of reactive biomass, an increase in the rates, such as seen in the lower dose experiments, points toward an increase in biomass.

The reaction rate data also presents the idea of a possible threshold concentration below which adaptation of the bacteria may occur. It appears that the threshold concentration was around 0.5 mg L^{-1} for this system. When the biocide concentration increases past this threshold, the bacteria no longer have the capacity to handle the biocide and are killed. At concentrations lower than the threshold, they can adapt to the threatening environment and increase the amount of reactive biomass. This increase in reactive biomass in turn causes an

increase in the overall reaction rate.

The reaction rate curves were integrated to determine the amount of chlorine reacted during the dosing period. For the 4 mg L^{-1}, 2 hr dose experiment presented, approximately 6.5 mg of monochloramine were reacted. This value jumped up to 27.5 mg for the 2 mg L^{-1}, 8 hr dose experiment. Similar results were found for the other high and low dose concentration experiments. These results indicate that the first order approximation used was reasonable for the high dose experiments, but not the low dose experiments. The reaction appeared to be independent of the concentration of monochloramine for low doses. A zero order approximation would likely have been a better estimation for these experiments.

Transport Limitation

Transport limitation of monochloramine into the biofilm was not a significant factor in this experimental system. An observable modulus comparing the rates of reaction and diffusion was never greater than 2.415. This maximum occurred during the 2 mg L^{-1}, 4 hr dose experiment when the effluent total chlorine detected was decreasing. The observable modulus values were generally quite small (avg. 0.381 ± 0.098) indicating that diffusion was not limiting. Transport limitation can not fully explain the reduction in efficacy of monochloramine in this study. This result contrasts recent findings of significant transport limitation using the more reactive biocide, chlorine. Transport limitation was demonstrated

to reduce the efficacy of chlorine in artificial biofilms (Xu *et al.*, 1996).

Mathematical Model Studies

The modeling simulations performed with AQUASIM could capture the basic overall trends seen in the experiments. They could not, however, fully fit many of the individual features observed experimentally. The viable and total cell reductions, as well as the higher dose (4 mg L^{-1}) effluent total chlorine, were fit relatively well by the model. The model could not capture the slower regrowth seen for all experiments. It was unable to fit the effluent chlorine data for the lower dose (2 mg L^{-1}) experiments. The overall double dose experiments were not accurately fit. The parameters used for fitting one experiment were not able to predict the results seen for another. This difficulty limits the applicability of the model for broader studies.

Viable and Total Cells

The model fits for the viable and total cell data captured the trends seen experimentally. The model fit nearly the same reduction in viable cells as seen in each experiment. The reduction in total cells was also very close to what was observed. The fit regrowth of viable and total cells was always faster than what had occurred experimentally. If the slow regrowth seen experimentally resulted from the presented hypothesis, the model would not be able to match it. A physiological adaptation is not considered in the model.

A problem arose in attempting to use the same parameters for fitting different experimental data sets. Parameters had to be adjusted to fit each different dosing protocol. The changes were by as much as an order of magnitude for two of the three parameters. The k_{rxn} and Y_{bn} parameters varied greatly during the fitting procedures. The k_{dis} stayed relatively constant for all protocols. The k_{rxn} was large for the high dose experiments and decreased for the lower dose experiments. This drop indicated less reaction with the monochloramine was occurring. Experimental reaction rates support this observation. An opposite trend was seen with the parameter Y_{bn}. Y_{bn}, which is a yield coefficient for neutralizer, was low when a high dose of monochloramine was added to the system and high when a low dose was added. This result means that the biofilm was able to neutralize more monochloramine when it was exposed to a lower dose. These results probably indicate that biological variability or adaptation was not captured by the model.

Prediction of double dose experiments also presented a couple of problems. The first was in the timing of the doses. The experimental total cell number minimum was not the same as the predicted total cell minimum. If the time of the experimental minimum was used, the predicted total cells were already regrowing. Simulations were performed using the time of both the experimental and predicted minimums. The results obtained were relatively close, but the effect may be important for determining the most effective protocol in other systems.

There was also difficulty in using the model to accurately fit the effect of the second dose of monochloramine on the viable and total cells. As discussed in the beginning of this chapter, the viable and total cell reduction after the second dose was not the same that typically occurred when using that concentration and duration of dose. This means that the parameters usually used for fitting the effect of the dose were no longer applicable. A different set of parameters was needed for reliable fit of the second dose. Parameters obtained for these second doses showed a drop in the k_{rxn} and an increase in Y_{bn} over what was found before. The second dose thus caused a decrease in the reaction of monochloramine and an increase in the amount being neutralized. The difference in parameters for the first and second doses made an overall fit basically impossible. The effect of each dose could be fit separately, but not together. The presented hypothesis, which may explain the lessened effect of monochloramine after the second dose, was not modeled.

Effluent Total Chlorine

The effluent total chlorine was fit by the model for each experiment. The model viewed the effluent total chlorine as the concentration of monochloramine in the bulk liquid compartment. The model generally fit the total chlorine breakthrough curves very well. It was even able to capture the delay in concentration increase at the beginning of the dose duration seen experimentally. The exception was seen when the model tried to predict the

effluent total chlorine for the low dose concentration (2 mg L^{-1}) experiments. These experiments had a fast peak and then continual decrease in total chlorine through the rest of the dose. The model could not fit this type of breakthrough curve. The model fits could be made to obtain the low effluent concentrations seen, but the early peaks were not attainable. The fits always had the concentrations increasing until the end of the dose. This could again be explained by a physiological change in the *P. aeruginosa* that the model structure is currently not capable of handling.

Transport Limitation

Transport limitation of monochloramine into the biofilm was examined with the model by predicting concentration gradients at various times during the dosing period. These gradients show almost complete penetration of the monochloramine to the biofilm substratum. There was some decrease in concentration seen at the substratum for the lower dose experiments. This decrease, however, was less than 0.05 mg L^{-1} or 11 percent. The model predictions agree with the results obtained from calculating the observable moduli from experimental data. Transport limitation was, therefore, not the reason for the ineffectiveness of monochloramine in controlling the biofilm.

CONCLUSIONS

The results from this research involving treatment of *P. aeruginosa* biofilms with monochloramine have led to the following conclusions:

1) There was a substantially greater reduction in viable cells than in total cells due to treatment.
2) Transport limitation can not explain the reduced efficacy of monochloramine for treating biofilms.
3) A more concentrated, shorter dose of monochloramine was more effective than the same amount of monochloramine delivered at a lower concentration over a longer period of time.
4) Experimental and modeling results point toward a physiological response by the bacteria making them less susceptible to disinfection.
5) Each experiment had to be modeled separately with AQUASIM. The fit parameters for one experiment were not applicable for another.
6) The model and experiments both support a timed dose strategy for efficient control of biofilms. More experimental work and further development of the model are needed to obtain the goal of an efficient dosing protocol.

RECOMMENDATIONS FOR FUTURE WORK

Further experimental and mathematical modeling work could support and strengthen the results obtained in this biofilm control study.

Expansion of this research from the relatively simple, single species system used is needed. Biofilm systems outside of the laboratory environment are usually more complex, containing multiple species and abiotic material, and are subject to variable environmental conditions. The next step might be to perform an evaluation using a mixed culture biofilm.

The hypothesis presented in this work of a physiological adaptation by the bacteria after being exposed to a biocide is another area needing investigation. Many of the experimental observations point toward this occurring in the system. This future investigation should include looking directly at physiological changes, such as metabolic and structural changes, which may be induced by the biocide. These changes may be identifiable at the genetic level. There may be up or down regulation of specific genes in the biofilm bacteria after coming in contact with the biocide. Knowing whether such changes are happening and how they occur may be vital to designing efficient biofilm control strategies.

The mathematical model used for this research should be modified. It could not fully capture the experimental results at this time. The modifications needed and implementation of these modifications hinge on the future experimental work in more complex systems and the physiological adaptation investigation.

NOMENCLATURE

A	biofilm surface area (m^{-2})
B	concentration of biocide ($g\ m^{-3}$)
D_b	diffusion coefficient of biocide in water ($m^2\ d^{-1}$)
D_s	diffusion coefficient of substrate in water ($m^2\ d^{-1}$)
k_d	detachment rate coefficient ($m^{-1}\ d^{-1}$)
k_{dis}	biocide disinfection rate coefficient ($m^3\ g^{-1}\ d^{-1}$)
k_{rxn}	biocide reaction rate coefficient ($m^3\ g^{-1}\ d^{-1}$)
K_s	substrate Monod half-saturation coefficient ($g\ m^{-3}$)
L_f	biofilm thickness (m)
L_L	liquid layer thickness (m)
N	concentration of neutralizer ($g\ m^{-3}$)
Q	volumetric flow rate ($m^3\ d^{-1}$)
r_B	overall reaction rate of biocide with biofilm ($g\ d^{-1}$)
R_{OBS}	overall biocide removal rate in liquid ($g\ m^{-3}\ d^{-1}$)
S	concentration of substrate ($g\ m^{-3}$)
t	time (d)
t_b	duration of biocide dose, $t_b = t_2 - t_1$ (d)
t_1	time of initiation of biocide dose (d)
t_2	time of cessation of biocide dose (d)
v	cell advective velocity ($m\ d^{-1}$)
V	volume of bulk liquid compartment (m^3)
x_A	live cell volume fraction
X_A	concentration of live cells in suspension ($g\ m^{-3}$)
x_I	dead cell volume fraction
X_I	concentration of dead cells in suspension ($g\ m^{-3}$)
x_T	cell fraction of total biofilm volume
Y_{bn}	yield coefficient of biocide consumed per neutralizer ($g\ g^{-1}$)
Y_{xs}	yield coefficient of biomass on substrate ($g\ g^{-1}$)
z	distance coordinate normal to substratum (m)
ρ_x	cell intrinsic density ($g\ m^{-3}$)
τ	biofilm/bulk fluid effective diffusivity ratio
Φ	observable modulus
μ_{MAX}	maximum specific growth rate (d^{-1})
i	influent value
$\circ$	initial value
$*$	bulk fluid value

REFERENCES CITED

REFERENCES CITED

Al-Hoti, B., Waite, T., and Chow, W. 1990. Development and calibration of a model for predicting optimum chlorination scenarios for biofouling control. pp. 521-534. In R. L. Jolley, L. W. Condie, J. D. Johnson, S. Katz, R. A. Minear, J. S. Mattice, and V. A. Jacobs (eds.), Water chlorination: Chemistry, environmental impact and health effects, Vol. 6. Lewis Publishers, Chelsea, MI.

Bailey, J. E. and Ollis, D. F. 1977. Biochemical engineering fundamentals, 1st Ed. Mc-Graw Hill, Inc., Englewood Cliffs, NJ.

Bakke, R., Trulear, M. G., Robinson, J. A., and Characklis, W. G. 1984. Activity of *Pseudomonas aeruginosa* in biofilms: Steady state. *Biotechnol. Bioeng.* 26: 1418-1424.

Biswas, P., Lu, C., and Clark, R. M. 1993. A model for chlorine concentration decay in pipes. *Wat. Res.* 27: 1715-1724.

Bremer, P. J. and Geesey, G. G. 1991. Laboratory-based model of microbiologically induced corrosion of copper. *Appl. Environ. Microbiol.* 57: 1956-1962.

Brock, T. D. and Madigan, M. T. 1991. Biology of microorganisms, 6th Ed. Prentice-Hall, Inc., Englewood Cliffs, NJ.

Brown, M. R. W. and Gilbert, P. 1993. Sensitivity of biofilms to antimicrobial agents. *J. Appl. Bacteriol. Symp. Suppl.* 74: 87S-97S.

Brözel, V. S., Pietersen, B., and Cloete, T. E. 1993. Adaptation of bacterial cultures to non-oxidising water treatment bactericides. *Water SA* 19: 259-262.

Camper, A. K. 1994. Coliform regrowth and biofilm accumulation in drinking water systems: A review. pp. 91-105. In G. G. Geesey, Z. Lewandowski, and H. -C. Flemming (eds.), Biofouling and biocorrosion in industrial water systems. Lewis Publishers, Boca Raton, FL.

Camper, A. K., McFeters, G. A., Characklis, W. G., and Jones, W. L. 1991. Growth kinetics of coliform bacteria under conditions relevant to drinking water distribution systems. *Appl. Environ. Microbiol.* 57: 2233-2239.

Chang, H. T. and Rittman, B. E. 1987. Mathematical modeling of biofilm on activated carbon. *Environ. Sci. Technol.* 21: 273-280.

Characklis, W. G. 1981. Fouling biofilm development: A process analysis. *Biotechnol. Bioeng.* 23: 1923-1960.

Characklis, W. G. 1990(a). Kinetics of microbial transformations. pp. 233-264. In W. G. Characklis and K. C. Marshall (eds.), Biofilms. John Wiley & Sons, Inc., NY.

Characklis, W. G. 1990(b). Microbial biofouling control. pp. 585-633. In W. G. Characklis and K. C. Marshall (eds.), Biofilms. John Wiley & Sons, Inc., NY.

Characklis, W. G. and Marshall, K. C. 1990. Biofilms: A basis for an interdisciplinary approach. pp. 3-15. In W. G. Characklis and K. C. Marshall (eds.), Biofilms. John Wiley & Sons, Inc., NY.

Chen, C. -I., Griebe, T., and Characklis, W. G. 1993. Biocide action of monochloramine on biofilm systems of *Pseudomonas aeruginosa*. *Biofouling.* 7: 1-17.

Christensen, B. E. and Characklis, W. G. 1990. Physical and chemical properties of biofilms. pp. 93-130. In W. G. Characklis and K. C. Marshall (eds.), Biofilms. John Wiley & Sons, Inc., NY.

Clesceri, L. S., Greenberg, A. E., and Trussell, R. R. (eds.). 1989. Standard methods for the examination of water and wastewater, 18th Ed. American Public Health Association, Washington, DC.

Coelhoso, I., Boaventura, R., and Rodrigues, A. 1992. Biofilm reactors: An experimental and modeling study of wastewater denitrification in fluidized-bed reactors of activated carbon particles. *Biotechnol. Bioeng.* 40: 625-633.

Costerton, J. W., Cheng, K. -J., Geesey, G. G., Ladd, T. I., Nickel, J.C., Dasgupta, M., and Marrie, T. J. 1987. Bacterial biofilms in nature and disease. *Ann. Rev. Microbiol.* 41: 435-464.

de Beer, D., Srinivasan, R., and Stewart, P. S. 1994. Direct measurement of chlorine penetration into biofilms during disinfection. *Appl. Environ. Microbiol.* 60: 4339-4344.

Drury, W. J. 1992. Interactions of 1μm latex microbeads with biofilms. Ph. D. thesis. Montana State University, Bozeman, MT.

Flora, J. R. V., Suidan, M. T., Biswas, P., and Sayles, G. D. 1993. Modeling substrate transport into biofilms: Role of multiple ions and pH effects. J. Environ. Eng. 119: 908-930.

Flora, J. R. V., Suidan, M. T., Biswas, P., and Sayles, G. D. 1995(a). A modeling study of anaerobic biofilm systems: I. Detailed biofilm modeling. *Biotechnol. Bioeng.* 46: 43-53.

Flora, J. R. V., Suidan, M. T., Biswas, P., and Sayles, G. D. 1995(b). A modeling study of anaerobic biofilm systems: II. Reactor modeling. *Biotechnol. Bioeng.* 46: 54-61.

Forster, C. F., Boyes, A. P., Hay, B. A., and Butt, J. A. 1986. An aerobic fluidised bed reactor for wastewater treatment. *Chem. Eng. Res. Des.* 64: 425-430.

Geesey, G. G., Bremer, P. J., Fischer, W. R., Wagner, D., Keevil, C. W., Walker, J., Chamberlain, A. H. L., and Angell, P. 1994. Unusual types of pitting corrosion of copper tubes in potable water systems. pp. 243-263. In G. G. Geesey, Z. Lewandowski, and H. -C. Flemming (eds.), Biofouling and biocorrosion in industrial water systems. Lewis Publishers, Boca Raton, FL.

Geesey, G. and Jang, L. 1989. Extracellular polymers for metal binding. pp. 223-247. In H. L. Ehrlich and C. L. Brierley (eds.), Microbial mineral recovery. Mc-Graw-Hill, Inc., NY.

Gjaltema, A., Arts, P. A. M., van Loosdrecht, M. C. M., Kuenen, J. G., and Heijnen, J. J. 1994. Heterogeneity of biofilms in rotating annular reactors: Occurrence, structure, and consequences. *Biotechnol. Bioeng.* 44: 194-204.

Griebe, T., Chen, C. -I., Srinivasan, R., and Stewart, P. S. 1994. Analysis of biofilm disinfection by monochloramine and free chlorine. pp. 151-161. In G. G. Geesey, Z. Lewandowski, and H. -C. Flemming (eds.), Biofouling and biocorrosion in industrial water systems. Lewis Publishers, Boca Raton, FL.

Gristina, A. G. and Costerton, J. W. 1985(a). Bacterial adherence to biomaterials and tissue. *J. Bone and Joint Surg.* 67-A: 264-273.

Gristina, A. G., Price, J. L., Hobgood, C. D., Webb, L. X., and Costerton, J. W. 1985(b). Bacterial colonization of percutaneous sutures. *Surg.* 98: 12-18.

Gujer W. and Wanner, O. 1990. Modeling mixed population biofilms. pp. 397-443. In W. G. Characklis and K. C. Marshall (eds.), Biofilms. John Wiley & Sons, Inc., NY.

Hamilton, M. A. 1991. Model validation: An annotated bibliography. *Commun. Statist.-Theory Meth.* 20: 2207-2266.

Jang, L. K., Brand, W., Resong, M., Mainieri, W., and Geesey, G. G. 1990. Feasibility of using alginate to absorb dissolved copper from aqueous media. *Environ. Prog.* 9: 269-274.

Jones, W. L., Dockery, J. D., Vogel, C. R., and Sturman, P. J. 1993. Diffusion and reaction within porous packing media: A phenomenological model. *Biotechnol. Bioeng.* 41:947-956.

Krieg, N. R., and Holt, J. G. (eds.). 1984. Bergey's manual of systematic bacteriology, Vol. 1. The Williams and Wilkins Company, Baltimore, MD.

LeChevallier, M. W., Cawthon, C. D., and Lee, R. G. 1988. Inactivation of biofilm bacteria. *Appl. Environ. Microbiol.* 54: 2492-2499.

Lee, W., Lewandowski, Z., Characklis, W. G., and Nielsen, P. H. 1994. Microbial corrosion of mild steel in a biofilm system. pp. 205-211. In G. G. Geesey, Z. Lewandowski, and H. -C. Flemming (eds.), Biofouling and biocorrosion in industrial water systems. Lewis Publishers, Boca Raton, FL.

Miller, I. R., Freund, J. E., and Johnson, R. A. 1990. Probability and statistics for engineers, 4th Ed. Prentice-Hall, Inc., Englewood Cliffs, NJ.

Murga, R., Stewart, P. S., and Daly, D. 1995. Quantitative analysis of biofilm thickness variability. *Biotechnol. Bioeng.* 45: 503-510.

Nichols, W. W. 1989. Susceptibility of biofilms to toxic compounds. pp. 321-331. In W. G. Characklis and P. A. Wilderer (eds.), Structure and function of biofilms. John Wiley & Sons, Inc., New York.

Nichols, W. W., Dorrington, S. M., Slack, M. P. E., and Walmsley, H. L. 1988. Inhibition of tobramycin diffusion by binding to alginate. *Antimicrob. Agents Chemother.* 32: 518-523.

Nichols, W. W., Evans, M. J., Slack, M. P. E., and Walmsley, H. L. 1989. The penetration of antibiotics into aggregates of mucoid and non-mucoid *Pseudomonas aeruginosa*. *J. Gen. Microbiol.* 135: 1291-1303.

Nickel, J. C., Wright, J. B., Ruseska, I., Marrie, T. J., Whitfield, C., and Costerton, J. W. 1985. Antibiotic resistance of *Pseudomonas aerginosa* colonizing a urinary catheter in vitro. *Eur. J. Clin. Microbiol.* 4: 213-218.

Norberg, A. and Rydin, S. 1984. Development of a continuous process for metal accumulation by *Zoogloea ramigera. Biotechnol. Bioeng.* 26: 265-268.

Perry, R. H., Green, D. W., and Maloney, J. O. (eds.). 1984. Perry's chemical engineers' handbook, 6th Ed. Mc-Graw-Hill, Inc., NY.

Peyton, B. M. 1992. Kinetics of biofilm detachment. Ph. D. thesis. Montana State University, Bozeman, MT.

Reichert, P. 1994(a). AQUASIM - A tool for simulation and data analysis of aquatic systems. *Wat. Sci Tech.* 30: 21-30.

Reichert, P. 1994(b). Concepts underlying a computer program for the identification and simulation of aquatic systems. Swiss Federal Institute for Environmental Science and Technology (EAWAG), CH-8600 Dübendorf, Switzerland.

Rittman, B. E. and Manem, J. A. 1992. Development and experimental evaluation of a steady-state, multispecies biofilm model. *Biotechnol. Bioeng.* 39: 914-922.

Rittman, B. E. and McCarty, P. L. 1980. Model of steady-state-biofilm kinetics. *Biotechnol. Bioeng.* 22: 2343-2357.

Robinson, J. A., Trulear, M. G., and Characklis, W. G. 1984. Cellular reproduction and extracellular polymer formation by *Pseudomonas aeruginosa* in continuous culture. *Biotechnol. Bioeng.* 26: 1409-1417.

Rossman, L. A., Clark, R. M., and Grayman, W. M. 1994. Modeling chlorine residuals in drinking-water distribution systems. *J. Environ. Eng.* 120: 803-820.

Ryhiner, G., Petrozzi, S., and Dunn, I. J. 1988. Operation of a three-phase biofilm fluidized sand bed reactor for aerobic wastewater treatment. *Biotechnol. Bioeng.* 32: 677-688.

Skowlund, C. T. 1990. Effect of biofilm growth on steady-state biofilm models. *Biotechnol. Bioeng.* 35: 502-510.

Skowlund, C. T. and Kirmse, D. W. 1989. Simplified models for packed-bed biofilm reactors. *Biotechnol. Bioeng.* 33: 164-172.

Stewart, P. S. 1993. A model of biofilm detachment. *Biotechnol. Bioeng.* 41: 111-117.

Stewart, P. S. 1994. Biofilm accumulation model that predicts antibiotic resistance of *Pseudomonas aeruginosa* biofilms. *Antimicrob. Agents Chemother.* 38: 1052-1058.

Stewart, P. S., Hamilton, M. A., Goldstein, B. R., and Schneider, B. T. 1996. Modeling biocide action against biofilms. *Biotechnol. Bioeng.* 49: 445-455.

Stewart, P. S., Peyton, B. M., Drury, W. J., and Murga, R. 1993. Quantitative observations of heterogeneities in *Pseudomonas aeruginosa* biofilms. *Appl. Env. Microbiol.* 59: 327-329.

Suidan, M. T. 1986. Performance of deep biofilm reactors. *J. Environ. Eng.* 112: 78-93.

Trulear, M. G. 1983. Cellular reproduction and extracellular polymer formation in the development of biofilms. Ph. D. thesis. Montana State University, Bozeman, MT.

van der Wende, E. 1991. Biocide action of chlorine on *Pseudomonas aeruginosa* biofilm. Ph. D. thesis. Montana State University, Bozeman, MT.

van der Wende, E. and Characklis, W. G. 1990. Biofilms in potable water distribution systems. pp. 249-268. In G. A. McFeters (ed.), Drinking water microbiology. Springer-Verlag, NY.

van der Wende, E., Characklis, W. G., and Smith, D. B. 1989. Biofilms and bacterial drinking water quality. *Wat. Res.* 23: 1313-1322.

Videla, H. A. and Characklis, W. G. 1992. Biofouling and microbially influenced corrosion. *Int. Biodet. Biodegrad.* 29: 195-212.

Wanner, O., Cunningham, A. B., and Lundman, R. 1995. Modeling biofilm accumulation and mass transport in a porous medium under high substrate loading. *Biotechnol. Bioeng.* 47: 703-712.

Wanner, O. and Reichert, P. 1996. Mathematical modeling of mixed-culture biofilms. *Biotechnol. Bioeng.* 49: 172-184.

Westrin, B. A. and Axelsson, A. 1991. Diffusion in gels containing immobilized cells: a critical review. *Biotechnol. Bioeng.* 38: 439-446.

Xu, X., Stewart, P. S., and Chen, X. 1996. Transport limitation of chlorine disinfection of *Pseudomonas aeruginosa* entrapped in alginate beads. *Biotechnol. Bioeng.* 49: 93-100.

Zelver, N. 1979. Biofilm development and associated energy losses in water conduits. M. S. thesis. Rice University, Houston, TX.

Zhou, H., Smith, D W., and Stanley, S. J. 1994. Modeling of dissolved ozone concentration profiles in bubble columns. *J. Environ. Eng.* 120: 821-840.

APPENDICES

APPENDIX A

Annular Reactor Characteristics

SPECIFICATION:	DIMENSION:
Outer cylinder:	
wet height	220 mm
diameter	113 mm
vertical wet surface area	78100 mm^2
horizontal wet surface area	10050 mm^2
total wet surface area	88150 mm^2
Inner cylinder:	
wet height	177 mm
diameter	102 mm
vertical wet surface area	56700 mm^2
horizontal wet surface area	16000 mm^2
total wet surface area	72700 mm^2
Draft tubes:	
number	4
length	180 mm
diameter	10 mm
surface area	23100 mm^2
angle of inclination	80°
Slides:	
number	12
length	220 mm
width	17 mm
thickness	0.5 mm
wet surface area (one slide)	3740 mm^2
Reactor:	
total wet surface area	184000 mm^2
total slide surface area	44800 mm^2
liquid volume	596000 mm^3
total surface/volume ratio	0.31 mm^{-1}
width of annular gap	5.5 mm

APPENDIX B

Viable and Total Cell Data

Experiment #3
Dose concentration: 4 mg L^{-1}
Dose duration: 2 hr

Table 10. Exp. #3: Viable and total cell mean counts.

Sampling Time, hr	Viable Cells, cfu m^{-2}	Total Cells, cells m^{-2}
0.0	1.85e+12	4.05e+11
0.25	2.20e+12	6.68e+11
0.5	2.27e+10	8.13e+11
1.0	1.04e+8	5.88e+11
2.0	5.64e+8	9.55e+11
4.0	2.48e+8	9.17e+11
6.75	4.67e+8	1.60e+12
9.33	5.99e+8	4.46e+11
22.33	1.32e+9	7.86e+10
34.33	6.92e+9	3.95e+10
48.33	2.35e+10	1.18e+11
98.33	5.12e+12	2.48e+12

Experiment #4
Dose concentration: 4 mg L^{-1}
Dose duration: 2 hr

Table 11. Exp. #4: Viable and total cell mean counts.

Sampling Time, hr	Viable Cells, cfu m^{-2}	Total Cells, cells m^{-2}
0.0	2.70e+12	7.07e+11
0.25	3.17e+12	7.46e+11
0.5	2.01e+12	1.40e+12
1.0	1.61e+11	8.51e+11
2.0	1.30e+9	4.84e+11
4.0	9.52e+7	7.99e+11
6.0	1.23e+9	4.84e+11
9.0	4.91e+8	8.12e+11
21.0	1.62e+9	1.85e+11
34.0	1.56e+10	4.32e+10
54.25	1.13e+11	4.71e+10
102.0	4.49e+12	7.59e+11

Experiment #6
Dose concentration: 0 mg L^{-1}
Dose duration: 2 hr

Table 12. Exp. #6: Viable and total cell mean counts.

Sampling Time, hr	Viable Cells, cfu m^{-2}	Total Cells, cells m^{-2}
0.0	1.42e+12	2.00e+12
0.5	1.31e+12	1.71e+12
1.0	1.89e+12	2.43e+12
2.0	1.40e+12	1.71e+12
4.33	4.27e+12	2.54e+12
6.33	1.03e+12	1.51e+12
12.67	3.29e+12	3.19e+12
24.0	3.49e+12	3.72e+12
36.33	2.47e+12	3.29e+12
49.58	4.27e+12	4.15e+12
73.33	1.24e+12	1.71e+12
84.33	1.68e+12	2.29e+12

Experiment #10
Dose concentration: 2 mg L^{-1}
Dose duration: 4 hr

Table 13. Exp. #10: Viable and total cell mean counts.

Sampling Time, hr	Viable Cells, cfu m^{-2}	Total Cells, cells m^{-2}
0.0	3.70e+12	2.24e+12
0.5	1.93e+12	2.45e+12
1.0	1.66e+12	2.74e+12
2.0	1.31e+12	3.08e+12
4.0	1.51e+12	1.71e+12
6.0	1.44e+12	1.85e+12
9.5	3.01e+12	2.38e+12
22.0	3.47e+12	3.02e+12
31.33	2.96e+12	3.29e+12
55.33	2.74e+12	2.50e+12
80.33	2.04e+12	2.65e+12

Experiment #12
Dose concentration: 2 mg L^{-1}
Dose duration: 8 hr

Table 14. Exp. #12: Viable and total cell mean counts.

Sampling Time, hr	Viable Cells, cfu m^{-2}	Total Cells, cells m^{-2}
0.0	5.73e+12	2.22e+13
1.0	3.87e+12	5.26e+12
2.0	3.41e+12	6.27e+12
4.0	2.71e+12	4.74e+12
6.0	2.63e+12	3.13e+12
8.17	1.16e+12	3.42e+12
12.17	6.59e+11	3.61e+12
24.17	3.07e+12	4.22e+12
49.0	3.50e+12	4.29e+12
77.58	3.74e+12	6.72e+12
101.58	3.67e+12	5.39e+12

Experiment #14
Dose concentration: 4 mg L^{-1}
Dose duration: 4 hr

Table 15. Exp. #14: Viable and total cell mean counts.

Sampling Time, hr	Viable Cells, cfu m^{-2}	Total Cells, cells m^{-2}
0.0	2.97e+12	4.74e+12
0.5	7.97e+10	5.43e+12
1.0	5.20e+9	3.93e+12
2.0	7.48e+8	4.85e+12
4.0	2.31e+8	2.17e+12
6.0	2.25e+8	1.43e+12
10.25	5.22e+8	6.99e+11
22.0	1.56e+7	8.56e+11
32.25	7.45e+7	1.27e+12
57.5	1.73e+10	1.10e+12
100.0	2.05e+11	1.21e+12
130.0	9.34e+11	5.77e+12

Experiment #17
Time between doses: 40 hr
1st dose concentration: 4 mg L^{-1}
1st dose duration: 2 hr
2nd dose concentration: 4 mg L^{-1}
2nd dose duration: 2 hr

Table 16. Exp. #17: Viable and total cell mean counts.

Sampling Time, hr	Viable Cells, cfu m^{-2}	Total Cells, cells m^{-2}
0.0	3.47e+12	5.58e+12
1.0	1.44e+12	8.72e+12
15.0	2.38e+9	3.52e+12
39.5	2.10e+10	2.15e+12
42.0	1.15e+9	1.27e+12
45.0	4.82e+8	5.50e+11
52.0	4.68e+8	5.60e+11
64.0	5.43e+9	7.46e+11
90.0	5.09e+10	5.69e+11
103.5	4.46e+11	3.73e+11
126.0	1.21e+12	3.22e+12
176.0	1.45e+12	5.92e+12

Experiment #18
Time between doses: 0 hr
1st dose concentration: 2 mg L^{-1}
1st dose duration: 4 hr
2nd dose concentration: 4 mg L^{-1}
2nd dose duration: 2 hr

Table 17. Exp. #18: Viable and total cell mean counts.

Sampling Time, hr	Viable Cells, cfu m^{-2}	Total Cells, cells m^{-2}
0	5.81e+12	7.92e+12
0.5	1.98e+12	6.66e+12
2.0	2.99e+12	7.30e+12
3.75	9.71e+11	4.94e+12
5.0	8.27e+10	6.54e+12
6.0	1.15e+10	5.53e+12
8.25	7.57e+10	6.56e+12
11.0	1.95e+10	5.37e+12
24.0	1.76e+10	1.54e+12
48.0	4.98e+10	2.18e+12
72.0	5.97e+11	1.83e+12
114.0	8.65e+12	5.24e+12

Experiment #19
Time between doses: 60 hr
1st dose concentration: 4 mg L^{-1}
1st dose duration: 2 hr
2nd dose concentration: 4 mg L^{-1}
2nd dose duration: 2 hr

Table 18. Exp. #19: Viable and total cell mean counts.

Sampling Time, hr	Viable Cells, cfu m^{-2}	Total Cells, cells m^{-2}
0	1.15e+13	1.19e+13
2.0	4.55e+10	9.29e+12
4.0	1.85e+10	5.28e+12
14.0	3.69e+9	5.47e+12
26.0	6.34e+9	6.02e+12
59.5	9.22e+10	1.12e+12
62.0	1.00e+9	4.48e+11
65.0	3.54e+8	9.58e+11
72.0	3.14e+8	5.73e+11
85.0	4.83e+8	7.38e+11
118.5	2.05e+10	3.69e+11
147.0	3.51e+11	2.62e+12

Error Analysis

Table 19. The standard error of the means (SEM) for viable cells, total cells, and total chlorine (log scale for viable and total cells).

Experiment #	Viable Cells log(cfu m^{-2})		Total Cells, log(cells m^{-2})	Total Chlorine, mg L^{-1}
	2 Dilutions	3 Dilutions		
3	0.176	0.144	0.105	—
4	0.142	0.116	0.066	—
6	0.148	0.121	0.098	—
10	0.136	—	0.068	—
12	0.117	0.096	0.071	—
14	0.162	0.132	0.098	—
17	0.109	0.089	0.086	—
18	0.192	0.157	0.075	0.0226
19	0.107	0.087	0.093	0.0232

APPENDIX C

Effluent Total Chlorine Data

Experiment #3
Dose concentration: 4 mg L^{-1}
Dose duration: 2 hr

Table 20. Exp. #3: Effluent total chlorine.

Sampling Time, min	Absorbance at 515 nm	Total Chlorine, mg L^{-1}
0	0.033	0.137
5	0.041	0.171
11	0.041	0.171
13	0.048	0.200
14	0.054	0.225
15	0.046	0.192
20	0.064	0.267
34	0.081	0.337
40	0.347	1.446
60	0.805	3.354
82	1.007	4.195
100	1.142	4.757
122	1.257	5.237
135	1.066	4.441
155	0.032	0.133
195	0.015	0.062

Experiment #4
Dose concentration: 4 mg L^{-1}
Dose duration: 2 hr

Table 21. Exp. #4: Effluent total chlorine.

Sampling Time, min	Absorbance at 515 nm	Total Chlorine, mg L^{-1}
0	0.027	0.112
8	0.038	0.158
13	0.029	0.121
15	0.027	0.112
18	0.033	0.137
20	0.033	0.137
30	0.050	0.208
45	0.086	0.358
62	0.235	0.979
80	0.431	1.795
100	0.659	2.745
120	0.799	3.329
140	0.865	3.603
160	0.519	2.162
180	0.178	0.742
200	0.050	0.208
210	0.021	0.087

Experiment #10
Dose concentration: 2 mg L^{-1}
Dose duration: 4 hr

Table 22. Exp#10: Effluent total chlorine.

Sampling Time, min	Absorbance at 515 nm	Total Chlorine, mg L^{-1}
0	0.005	0.021
10	0.004	0.017
15	0.039	0.162
20	0.041	0.171
25	0.038	0.158
30	0.032	0.133
40	0.030	0.125
45	0.054	0.225
60	0.038	0.158
78	0.029	0.121
90	0.019	0.079
105	0.018	0.075
120	0.010	0.042
135	0.014	0.058
150	0.014	0.058
165	0.012	0.050
180	0.019	0.079
195	0.017	0.071
210	0.016	0.067
225	0.019	0.079
240	0.013	0.054
255	0.044	0.183
270	0.021	0.087
285	0.015	0.062
300	0.012	0.050
315	0.013	0.054
330	0.005	0.021

Experiment #12
Dose concentration: 2 mg L^{-1}
Dose duration: 8 hr

Table 23. Exp. #12: Effluent total chlorine.

Sampling Time, min	Absorbance at 515 nm	Total Chlorine, mg L^{-1}
0	0.029	0.121
10	0.075	0.312
15	0.095	0.396
20	0.110	0.458
30	0.120	0.500
45	0.111	0.462
60	0.109	0.454
90	0.106	0.442
120	0.048	0.200
150	0.040	0.167
180	0.025	0.104
210	0.022	0.092
240	0.017	0.071
270	0.023	0.096
300	0.050	0.208
330	0.018	0.075
360	0.015	0.063
390	0.009	0.038
420	0.008	0.033
450	0.002	0.008
490	0.001	0.006

Experiment #14
Dose concentration: 4 mg L^{-1}
Dose duration: 4 hr

Table 24. Exp. #14: Effluent total chlorine.

Sampling Time, min	Absorbance at 515 nm	Total Chlorine, mg L^{-1}
0	0.017	0.071
5	0.082	0.342
10	0.162	0.675
15	0.218	0.908
20	0.264	1.10
25	0.307	1.28
30	0.365	1.52
45	0.601	2.50
60	0.754	3.14
75	0.852	3.55
90	0.925	3.85
105	0.919	3.83
135	0.894	3.72
150	0.890	3.71
165	0.931	3.88
180	0.884	3.68
210	0.912	3.80
240	0.890	3.71
255	0.486	2.02
285	0.118	0.492
300	0.060	0.250
330	0.022	0.092
390	0.018	0.075

Experiment #17

Time between doses: 40 hr
1st dose concentration: 4 mg L^{-1}
1st dose duration: 2 hr
2nd dose concentration: 4 mg L^{-1}
2nd dose duration: 2 hr

Table 25. Exp. #17: Effluent total chlorine.

Sampling Time, min	Absorbance at 515 nm	Total Chlorine, mg L^{-1}		Sampling Time, min	Absorbance at 515 nm	Total Chlorine, mg L^{-1}
0	0.031	0.129		2400	0.016	0.067
5	0.042	0.175		2405	0.056	0.233
10	0.064	0.267		2410	0.161	0.671
15	0.080	0.333		2415	0.260	1.083
20	0.087	0.362		2420	0.343	1.429
25	0.092	0.383		2425	0.434	1.808
30	0.114	0.475		2430	0.491	2.045
45	0.143	0.596		2445	0.584	2.433
60	0.195	0.812		2460	0.662	2.758
75	0.368	1.533		2475	0.687	2.862
90	0.546	2.275		2490	0.720	2.999
105	0.703	2.929		2505	0.735	3.062
120	0.754	3.141		2520	0.778	3.241
135	0.766	3.191		2535	0.731	3.045
145	0.522	2.175		2550	0.380	1.583
150	0.319	1.329		2565	0.152	0.633
165	0.171	0.712		2580	0.078	0.325
180	0.103	0.429		2595	0.058	0.242
195	0.081	0.337		2610	0.020	0.083
210	0.046	0.192				
225	0.029	0.121				

Experiment #18
Time between doses: 0 hr
1st dose concentration: 2 mg L^{-1}
1st dose duration: 4 hr
2nd dose concentration: 4 mg L^{-1}
2nd dose duration: 2 hr

Table 26. Exp. #18: Effluent total chlorine.

Sampling Time, min	Absorbance at 515 nm	Duplicate Absorbance at 515 nm	Total Chlorine, mg L^{-1}	Duplicate Total Chlorine, mg L^{-1}
0	0.016		0.067	
5	0.042		0.175	
10	0.053		0.221	
15	0.065	0.059	0.271	0.246
20	0.089		0.371	
30	0.066		0.275	
45	0.048		0.200	
75	0.046		0.192	
105	0.042	0.054	0.175	0.225
135	0.055	0.057	0.229	0.237
165	0.061	0.061	0.254	0.254
195	0.030	0.033	0.125	0.137
210	0.074		0.308	
225	0.049		0.204	
245	0.086		0.358	
250	0.106	0.106	0.442	0.442
260	0.127		0.529	
270	0.167	0.158	0.696	0.658
285	0.184		0.767	
300	0.219		0.912	
315	0.364		1.516	
330	0.553	0.580	2.304	2.416
345	0.684		2.849	
375	0.714		2.974	
390	0.343	0.351	1.429	1.462
405	0.143		0.596	
420	0.054		0.225	
435	0.023		0.096	

Experiment #19
Time between doses: 60 hr
1st dose concentration: 4 mg L^{-1}
1st dose duration: 2 hr
2nd dose concentration: 4 mg L^{-1}
2nd dose duration: 2 hr

Table 27. Exp. #19: Effluent total chlorine – 1st dose.

Sampling Time, min	Absorbance at 515 nm	Duplicate Absorbance at 515 nm	Total Chlorine, mg L^{-1}	Duplicate Total Chlorine, mg L^{-1}
0	0.036	0.038	0.150	0.158
5	0.070		0.292	
10	0.079	0.101	0.329	0.421
15	0.096	0.107	0.400	0.446
20	0.097		0.404	
25	0.097	0.114	0.404	0.475
30	0.114		0.475	
45	0.143		0.596	
60	0.180		0.750	
75	0.194	0.183	0.808	0.762
90	0.414		1.725	
105	0.754	0.763	3.141	3.179
120	0.841		3.504	
135	0.578		2.408	
150	0.318		1.325	
165	0.150	0.160	0.625	0.667
180	0.093		0.387	
195	0.050		0.208	

Experiment #19

Time between doses: 60 hr
1st dose concentration: 4 mg L^{-1}
1st dose duration: 2 hr
2nd dose concentration: 4 mg L^{-1}
2nd dose duration: 2 hr

Table 28. Exp. #19: Effluent total chlorine – 2nd dose.

Sampling Time, min	Absorbance at 515 nm	Duplicate Absorbance at 515 nm	Total Chlorine, mg L^{-1}	Duplicate Total Chlorine, mg L^{-1}
3600	0.028	0.018	0.117	0.075
3605	0.155		0.646	
3610	0.271	0.273	1.129	1.137
3615	0.371		1.546	
3620	0.450		1.875	
3625	0.528	0.539	2.200	2.245
3630	0.594		2.475	
3645	0.733		3.054	
3660	0.758	0.768	3.158	3.199
3675	0.806		3.358	
3690	0.868		3.616	
3705	1.002	1.004	4.174	4.183
3720	1.019		4.245	
3735	0.631		2.629	
3750	0.290	0.292	1.208	1.216
3765	0.141		0.587	
3780	0.075		0.312	
3795	0.052	0.038	0.217	0.158

APPENDIX D

Reaction Rate Data

Experiment #3
Dose concentration: 4 mg L^{-1}
Dose duration: 2 hr

Table 29. Exp. #3: Reaction rates.

Time, min	Total Chlorine, mg L^{-1}	dB/dt	Reaction Rate, mg min^{-1}
0	0.137	—	—
5	0.171	0.003	0.160
11	0.171	0.007	0.158
13	0.200	0.020	0.150
14	0.225	-0.004	0.163
15	0.192	-0.009	0.167
20	0.267	0.010	0.153
34	0.337	0.95	0.100
40	1.446	0.140	0.038
60	3.354	0.067	0.021
82	4.195	0.035	0.013
100	4.760	0.027	0.000
122	5.240	0.022	-0.013
135	4.440	-0.138	-0.060
155	0.133	-0.109	0.060
195	0.062	-0.002	-0.001

Experiment #4
Dose concentration: 4 mg L^{-1}
Dose duration: 2 hr

Table 30. Exp. #4: Reaction rates.

Time, min	Total Chlorine, mg L^{-1}	dB/dt	Reaction Rate, mg min^{-1}
0	0.112	—	—
8	0.158	-0.001	0.123
13	0.121	-0.006	0.128
15	0.112	0.002	0.123
18	0.137	0.004	0.121
20	0.137	0.004	0.121
30	0.208	0.009	0.116
45	0.358	0.023	0.103
62	0.979	0.041	0.072
80	1.795	0.046	0.043
100	2.745	0.038	0.017
120	3.329	0.022	0.009
140	3.603	0.014	0.004
160	2.162	-0.072	-0.027
180	0.742	-0.049	0.005
200	0.208	-0.019	0.005
210	0.087	-0.012	0.004

Experiment #10
Dose concentration: 2 mg L^{-1}
Dose duration: 4 hr

Table 31. Exp. #10: Reaction rates.

Time, min	Total Chlorine, mg L^{-1}	dB/dt	Reaction Rate, mg min^{-1}
0	0.021	—	—
10	0.017	0.014	0.055
15	0.162	0.015	0.050
20	0.171	-0.000	0.059
25	0.158	-0.004	0.061
30	0.133	-0.003	0.061
40	0.125	0.010	0.054
45	0.225	0.020	0.045
60	0.158	-0.003	0.061
78	0.121	-0.003	0.062
90	0.079	-0.002	0.063
105	0.075	-0.001	0.062
120	0.042	-0.001	0.063
135	0.058	0.001	0.062
150	0.058	-0.000	0.062
165	0.050	0.001	0.062
180	0.079	0.001	0.061
195	0.071	-0.000	0.062
210	0.067	0.000	0.062
225	0.079	-0.000	0.062
240	0.054	0.004	0.060
255	0.183	0.009	-0.011
270	0.087	-0.004	0.000
285	0.062	-0.001	-0.001
300	0.050	-0.000	-0.001
315	0.054	-0.001	-0.001
330	0.021	-0.002	0.001

Experiment #12
Dose concentration: 2 mg L^{-1}
Dose duration: 8 hr

Table 32. Exp. #12: Reaction rates.

Time, min	Total Chlorine, mg L^{-1}	dB/dt	Reaction Rate, mg min^{-1}
0	0.121	—	—
10	0.312	0.018	0.043
15	0.396	0.015	0.043
20	0.458	0.008	0.044
30	0.500	0.004	0.046
45	0.462	-0.002	0.050
60	0.454	-0.001	0.050
90	0.442	-0.004	0.052
120	0.200	-0.005	0.060
150	0.167	-0.002	0.060
180	0.104	-0.001	0.061
210	0.092	-0.001	0.061
240	0.071	0.000	0.062
270	0.096	0.002	0.060
300	0.208	0.004	0.055
330	0.075	-0.002	0.063
360	0.063	-0.001	0.062
390	0.038	-0.001	0.063
420	0.033	-0.001	0.063
450	0.008	-0.000	0.064
490	0.006	-0.000	0.000

Experiment #14
Dose concentration: 4 mg L^{-1}
Dose duration: 4 hr

Table 33. Exp. #14: Reaction rates.

Time, min	Total Chlorine, mg L^{-1}	dB/dt	Reaction Rate, mg min^{-1}
0	0.071	—	—
5	0.342	0.060	0.081
10	0.675	0.057	0.073
15	0.908	0.043	0.074
20	1.100	0.037	0.071
25	1.279	0.042	0.062
30	1.521	0.057	0.045
45	2.504	0.054	0.016
60	3.141	0.035	0.007
75	3.549	0.024	0.000
90	3.853	0.009	-0.001
105	3.828	-0.003	0.007
135	3.724	-0.002	0.010
150	3.708	0.005	0.006
165	3.878	-0.001	0.004
180	3.683	-0.005	0.013
210	3.799	0.000	0.006
240	3.708	-0.003	0.011
255	2.025	-0.082	-0.016
285	0.492	-0.034	0.004
300	0.250	-0.011	-0.002
330	0.092	-0.003	-0.001
390	0.075	-0.000	-0.002

Experiment #17

Time between doses: 40 hr
1st dose concentration: 4 mg L^{-1}
1st dose duration: 2 hr
2nd dose concentration: 4 mg L^{-1}
2nd dose duration: 2 hr

Table 34. Exp. #17: Reaction rates – 1st dose.

Time, min	Total Chlorine, mg L^{-1}	dB/dt	Reaction Rate, mg min^{-1}
0	0.129	—	—
5	0.175	0.014	0.114
10	0.267	0.016	0.110
15	0.333	0.010	0.112
20	0.362	0.005	0.113
25	0383	0.011	0.109
30	0.475	0.013	0.105
45	0.596	0.011	0.102
60	0.812	0.031	0.083
75	1.533	0.049	0.050
90	2.275	0.047	0.027
105	2.929	0.029	0.017
120	3.141	0.009	0.022
135	3.191	0.003	0.024
145	2.175	-0.135	0.011
150	1.329	-0.105	0.020
165	0.712	-0.030	-0.005
180	0.429	-0.013	-0.006
195	0.337	-0.008	-0.006
210	0.192	-0.007	-0.002
225	0.121	-0.005	-0.001

Experiment #17
Time between doses: 40 hr
1st dose concentration: 4 mg L^{-1}
1st dose duration: 2 hr
2nd dose concentration: 4 mg L^{-1}
2nd dose duration: 2 hr

Table 35. Exp. #17: Reaction rates – 2nd dose.

Time, min	Total Chlorine, mg L^{-1}	dB/dt	Reaction Rate, mg min^{-1}
2400	0.067	0.017	0.116
2405	0.233	0.060	0.085
2410	0.671	0.085	0.056
2415	1.083	0.076	0.048
2420	1.429	0.073	0.039
2425	1.808	0.062	0.033
2430	2.045	0.037	0.041
2445	2.433	0.024	0.036
2460	2.758	0.014	0.031
2475	2.862	0.008	0.032
2490	2.999	0.007	0.028
2505	3.062	0.008	0.025
2520	3.241	-0.001	0.025
2535	3.045	-0.013	0.038
2550	1.583	-0.080	-0.033
2565	0.633	-0.042	0.005
2580	0.325	-0.013	-0.003
2595	0.242	-0.008	-0.003
2610	0.083	-0.011	0.004

Experiment #18

Time between doses: 0 hr
1st dose concentration: 2 mg L^{-1}
1st dose duration: 4 hr
2nd dose concentration: 4 mg L^{-1}
2nd dose duration: 2 hr

Table 36. Exp. #18: Reaction rates.

Time, min	Total Chlorine, mg L^{-1}	dB/dt	Reaction Rate, mg min^{-1}
0	0.067	—	—
5	0.175	0.015	0.049
10	0.221	0.010	0.051
15	0.271	0.015	0.046
20	0.371	0.020	0.040
30	0.275	-0.007	0.060
45	0.200	-0.003	0.059
75	0.192	-0.000	0.058
105	0.175	0.001	0.058
135	0.229	0.001	0.056
165	0.254	-0.002	0.057
195	0.125	0.004	0.058
210	0.308	0.003	0.053
225	0.204	0.000	0.057
245	0.358	0.012	0.109
250	0.442	0.013	0.106
260	0.529	0.013	0.103
270	0.696	.011	0.099
285	0.767	0.007	0.099
300	0.912	0.025	0.084
315	1.516	0.046	0.052
330	2.304	0.044	0.028
345	2.849	0.020	0.025
375	2.974	0.004	0.030
390	1.429	-0.079	0.002
405	0.596	-0.040	0.005
420	0.225	-0.017	0.003
435	.096	-0.009	0.002

Experiment #19
Time between doses: 60 hr
1st dose concentration: 4 mg L^{-1}
1st dose duration: 2 hr
2nd dose concentration: 4 mg L^{-1}
2nd dose duration: 2 hr

Table 37. Exp. #19: Reaction rates – 1st dose.

Time, min	Total Chlorine, mg L^{-1}	dB/dt	Reaction Rate, mg min^{-1}
0	0.150	—	—
5	0.292	0.018	0.108
10	0.329	0.011	0.111
15	0.400	0.008	0.111
20	0.404	0.000	0.115
25	0.404	0.007	0.111
30	0.475	0.011	0.106
45	0.596	0.009	0.103
60	0.750	0.007	0.100
75	0.808	0.033	0.083
90	1.725	0.078	0.026
105	3.141	0.059	-0.008
120	3.504	0.024	0.001
135	2.408	-0.073	-0.034
150	1.325	-0.059	-0.007
165	0.625	-0.031	-0.001
180	0.387	-0.014	-0.004
195	0.208	-0.012	0.000

Experiment #19

Time between doses: 60 hr
1st dose concentration: 4 mg L^{-1}
1st dose duration: 2 hr
2nd dose concentration: 4 mg L^{-1}
2nd dose duration: 2 hr

Table 38. Exp. #19: Reaction rates – 2nd dose.

Time, min	Total Chlorine, mg L^{-1}	dB/dt	Reaction Rate, mg min^{-1}
3600	0.117	0.053	0.100
3605	0.646	0.101	0.055
3610	1.129	0.090	0.046
3615	1.546	0.075	0.042
3620	1.875	0.065	0.037
3625	2.200	0.060	0.030
3630	2.475	0.047	0.029
3645	3.054	0.023	0.024
3660	3.158	0.010	0.029
3675	3.358	0.015	0.019
3690	3.616	0.027	0.004
3705	4.174	0.021	-0.010
3720	4.245	0.005	-0.003
3735	2.629	-0.101	-0.024
3750	1.208	-0.068	0.002
3765	0.587	-0.030	-0.001
3780	0.312	-0.012	-0.003
3795	0.217	-0.006	-0.003